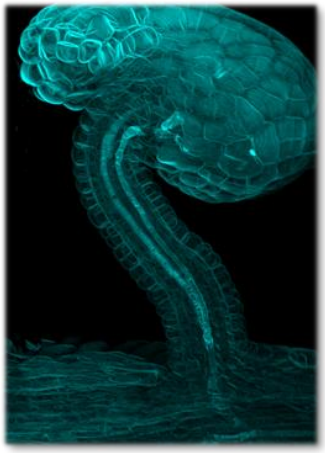

A multistep study to unveil the involvement of peptide signalling in STK-dependent pathways in *Arabidopsis thaliana*

Maria João Nogueira Ferreira

Biologia Funcional e Biotecnologia de Plantas

Departamento Biologia

2018

Orientador

Sílvia Coimbra, Professor auxiliar, FCUP

Coorientador

Maria Isabel Amorim, Professor auxiliar, FCUP

Coorientador

Tetsuya Higashiyama, Professor, ITbM, Nagoya University

Todas as correções determinadas pelo júri, e só essas, foram efetuadas.

O Presidente do Júri,

Porto, _____/_____/_____

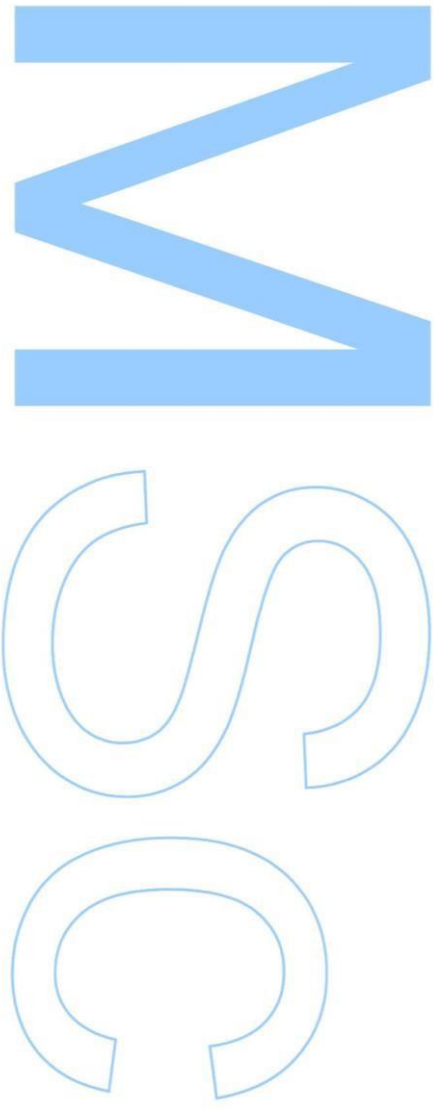

Acknowledgements

À Professora Sílvia Coimbra por me ter recebido no seu grupo e ter-me dado uma oportunidade incrível que indubitavelmente me fez crescer pessoalmente e profissionalmente. Obrigada pelo apoio durante este ano de tese. À Professora Isabel Amorim, agradeço-lhe por ter acreditado em mim e desafiado a entrar no mundo das plantas quando ainda não imaginava que iria seguir esse rumo. Obrigada pela ajuda durante estes anos.

Aos meus companheiros SPReDianos, obrigada pela ajuda prestada, pelos conselhos e ensinamentos!

À minha família por sempre me apoiarem em todas as decisões que tomo e serem um fator determinante nessas escolhas. Pais e tia, é verdade que tudo se torna mais fácil quando sabemos que temos uma rede pronta a amparar-nos de uma queda. Mesmo que seja no Japão!

Aos meus amigos, agradeço pela vossa paciência para comigo. Às vezes o stress fala mais alto, mas é uma mais valia ter pessoas com quem podemos partilhar as nossas frustrações. Susana, Márcio, Débora, Mariana, Patrício, Antero e Inês, obrigada pela companhia que me fizeram, mesmo com as 8/9 horas de diferença que existiam entre nós.

To professor Higashiyama, for accepting me in his group and contribute for a pleasant stay in Nagoya. Thank you for giving me the tools I needed for my work and for the advices regarding it. I feel very privileged for having met you, Professor.

To Hide, I know you don't like the word "supervisor", so thank you for your guidance. It really helped me to become more confident and independent in working at the lab. It was very helpful for my work to talk and discuss some topics with you. I can say it also contributed to my critical thinking skills. To Kazu, you were a great lab host! Thank you for introducing me to the lab, for the advices about my work, and for always answer to my questions (I know I could be annoying sometimes). To Bob, for sharing this 6 months experience with me. You were an amazing Japanese culture teacher and an even greater friend and lab partner (thank you for cheering me up with ice cream). You showed me that the scientist life is not easy, but it can be very rewarding. I also need to thank

Takuya for sharing his teachings with me and to Kimata for his advices about my transcriptome experience.

To Kathy, Tamiris and Paolo, for their support and friendship. Even though you were from another group, I felt we were from the same. Kathy you were a great deskmate and our “juicy” talks were a good escape from work. Tamiris and Paolo we must have another karaoke night!

To my share house friends, you really were an important part of my experience in Japan. Mifuyu, Matt and Sean, you taught me a lot about Japan and its society. I enjoyed spending time with you. Thank you for hearing my complaints! Tingting, Pim, Haruna, Waka and Sasuke, I am very happy for having met you. Thank you for the good talks, the walks and the tasty meals.

Por fim, mas não menos importante, um agradecimento especial à Diana por ter partilhado esta experiência comigo. Obrigada pela tua companhia e ajuda durante o tempo infinito em que eu estava na sala das plantas, por seres uma boa companheira de viagem e por não te importares de ouvir tantas canções!

Resumo

Nos óvulos das plantas com flor, os tecidos esporofíticos envolvem e protegem o saco embrionário. O estudo de óvulos com alterações nos tecidos esporofíticos demonstrou que existe uma comunicação entre o esporófito e o megagametófito, sendo esta importante para o desenvolvimento de sementes viáveis. Todavia, os processos subjacentes à coordenação célula-célula continuam pouco claros. A sinalização por péptidos é uma hipótese plausível visto ser um processo biológico já reportado na reprodução em plantas. Resultados recentes mostraram que os tecidos esporofíticos do óvulo, nomeadamente o funículo e os tegumentos, podem estar envolvidos na sinalização por péptidos, apesar de ainda não ter sido descrito nenhum par de péptido-recetor relacionado com os processos reprodutivos. *SEEDSTICK* (*STK*) é um gene que codifica um fator de transcrição, regulador mestre no desenvolvimento do óvulo e cuja expressão é maioritariamente nos tecidos esporofíticos do óvulo. O trabalho aqui apresentado pertence ao projeto SEXSEED e pretende desvendar o envolvimento da sinalização por péptidos nas vias controladas pelo STK.

No decorrer deste estudo, dados de transcriptómica obtidos de inflorescências *stk* foram cruzados com listas disponíveis de péptidos ricos em cisteínas (PRCs), que são um grupo de péptidos de plantas que assumem a função de ligantes, mediando aspetos relacionados com a reprodução em plantas. A análise confirmou que STK controla a expressão de genes que darão origem a PRCs. Várias metodologias foram testadas utilizando uma linha repórter para o STK, a fim de se obter dados transcriptómicos de tegumentos e funículo. Contudo, as experiências não foram bem-sucedidas. Um novo procedimento para o isolamento de células de funículo foi estabelecido e os dados de transcriptómica de funículos *stk* e da variedade selvagem (VS), após a fecundação ter ocorrido, estão a ser analisados. Para complementar o estudo de transcriptómica, foi também realizada uma análise fenotípica do *stk*. A orientação do crescimento do tubo polínico em pistilos *stk* foi examinada por azul de anilina e o comprimento do funículo *stk* e VS foi quantificado utilizando projeções de intensidade máxima de funículos. Esta análise fenotípica irá facilitar a interpretação dos dados de transcriptómica, permitindo relacionar o fenótipo com os genes desregulados identificados no mutante.

O presente trabalho foi importante, uma vez que surgiram novas informações quanto à rede de genes regulada pelo STK. A análise do sequenciamento de RNA de funículos

stk e VS será extremamente vantajosa para decifrar as funções do funículo controladas pelo STK e que são importantes para a correta formação da semente. É nosso intento que, num futuro próximo, esta análise culmine na transferência desta informação para espécies agrícolas de interesse económico.

Palavras-chave: *Arabidopsis thaliana*; bioinformática; comunicação célula-célula; funículo; sinalização por péptidos; *SEEDSTICK*; tegumentos; transcriptoma.

Abstract

In seed plant ovules, the sporophytic tissues surround and protect the embryo sac. The analysis of ovules with defects in the sporophytic tissues has shown that a communication between the sporophyte and megagametophyte exists and is important for the development of viable seeds. Nevertheless, the processes behind cell-to-cell coordination are still unclear. One plausible way could be by peptide signalling, a biological process already reported in plant's reproduction. Recent results showed that the ovule's sporophytic tissues, namely the funiculus and integuments, may be involved with peptide signalling, even though no pair of peptide-receptor related to the reproductive process has been described yet. *SEEDSTICK* (*STK*) encloses for a transcription factor, master regulator of ovule development and highly expressed in the ovule's sporophytic tissues. The work presented here by is part of the SEXSEED project and intends to disclose the involvement of peptide signalling in the pathways controlled by STK.

In the course of this study, transcriptomic data obtained from *stk* inflorescences was crossed with available lists of cysteine-rich peptides (CRPs), a group of plant peptide ligands which mediates aspects of plant's reproduction. The analysis confirmed that STK was controlling the expression of CRPs genes. Several methodologies were performed using a STK reporter line to obtain integuments and funiculus transcriptomic data, however the experiments were not succeeded. A new procedure for funiculus cells isolation was established and the transcriptomic data from *stk* and wild type (WT) funiculi, after fertilization took place and is now under analysis. To complement the transcriptomic study, a phenotypic analysis on *stk* was also performed. Pollen tube guidance in *stk* pistils was examined by aniline blue and both *stk* and WT funiculus length was quantified using maximum intensity projections of funiculi. This phenotypic analysis will facilitate the transcriptomic data interpretation, allowing to relate phenotype with the deregulated genes identified in the mutant.

This survey was of value since new information was discovered regarding the STK regulatory network. The high-throughput RNA-sequencing analysis of funiculi from *stk* and WT plants will be extremely helpful in deciphering the funiculus functions under the control of STK, important for a correct seed formation. Hopefully, in the near future, that will culminate in the transference of this information to agricultural crop species.

Keywords: *Arabidopsis thaliana*; bioinformatics; cell-to-cell communication; funiculus; integuments; peptide signalling; *SEEDSTICK*; transcriptome.

Index

List of figures and tables

List of abbreviations

ABS - Arabidopsis B Sister

ACT7 - ACTIN 7

AGP - ARABINOGALACTAN PROTEIN

BEL1 – BELL 1

BSA – Bovine serum albumin

CCG - CENTRAL CELL GUIDANCE

Col-0 - Columbia 0 variety

CRPs – Cysteine-rich peptides

CTR1 - CONSTITUTIVE TRIPLE RESPONSE 1

DAB – Decolorized aniline blue

DAPI - 4′,6-diamidino-2-phenylindole

DEFL – Defensin- like peptides

DEG – Differentially expressed genes

ECA1 - Early Culture Abundant 1 peptides

FACS – Fluorescence activated cell sorting

FANS - Fluorescence activated nuclei sorting

FDR – False discovery rate

FG – Female gametophyte

FIS2 - FERTILIZATION INDEPENDENT SEED 2

gDNA - genomic Deoxyribonucleic acid

GFP – Green fluorescent protein

INO – INNER NO OUTER

LTP - Lipid-transfer protein family

MES - 4-morpholineethanesulfonic acid

MMC - Megaspore mother cell

MPK - MITOGEN-ACTIVATED PROTEIN KINASE

mRNA - messenger Ribonucleic acid

MS - Murashige and Skoog media

NIB – Nuclei isolation buffer

NPB – Nuclei purification buffer

PCR - Polymerase chain reaction

PI - Propidium iodide

PT - Pollen tube

RALFs - Rapid alkalinization factors

RLK - Receptor-like kinase

RNA-seq – Ribonucleic acid sequencing

rRNA – ribossomal Ribonucleic acid

RT-PCR – Reverse transcriptase PCR

SAZ - Seed abscission zone

SC - Seed coat

SCPL41 - SERINE CARBOXYPEPTIDASE- LIKE 41

SHP – SHATERPROOF

SR2200 – SCRI Renaissance 2200 staining

STK - SEEDSTICK

SUS4 - SUCROSE SYNTHASE 4

TAA1 - TRYPTOPHAN AMINOTRANSFERASE OF ARABIDOPSIS 1

TF – Transcription factor

WT - Wild type

1. Introduction

1.1. Reproductive process in *Arabidopsis thaliana*

All land plants possess a life cycle with alternation of generations between a gametophyte, a haploid organism, and a sporophyte, a diploid organism (Lora *et al*., 2016). The sporophyte produces two types of spores, microspore and macrospore, which will give rise to microgametophyte and megagametophyte, respectively (Yadegari and Drews, 2004). The male gametophyte, also referred as pollen grain, develops inside the locus of the anther, which is part of the stamen (male reproductive organ). When mature, the pollen grain will be released, containing a vegetative cell that will form the pollen tube (PT) and a generative cell, which by mitosis will originate two male gametes (McCormick, 2004; Palanivelu and Tsukamoto, 2012). On the other hand, the female gametophyte, also known as embryo sac, is completely enveloped by the maternal sporophytic tissues, being found within the ovule, which in turn is localized inside the ovary. When completely formed, the embryo sac encages, besides other type of cells, two female gametes, the egg cell and central cell (Drews *et al.*, 1998; Yadegari and Drews, 2004).

Angiosperms share an interesting and important process called double fertilization, where two fertilizations occur simultaneously (Raghavan, 2003). This unique feature is a key process for seed development and consequently, formation of the next plant generation (Bleckmann *et al.*, 2014). The process (Figure 1) begins when the pollen grain contacts with the stigmatic cells, germinates and produces the PT. At that point, the PT grows between the walls of the stigmatic cells, into the style and across the extracellular matrix of the transmitting tract (Figure 1A) (Yadegari and Drews, 2004). Once near an ovule, the PT elongates along the surface of the funiculus (the stalk that supports the ovule), changing its direction abruptly to reach the micropyle - the ovule opening – accurately (Figure 1B) (Hülskamp *et al.*, 1995; Shimizu and Okada, 2000). After growing through the micropyle, the PT enters in the female gametophyte, penetrating one of the two synergid cells. There, the tip of the PT bursts, releasing the two male gametes, which will fuse one with the egg cell, originating the diploid zygote, while the other will fuse with the central cell giving rise to the triploid endosperm, that will nurture the embryo during its development (Dresselhaus, 2006; Hamamura *et al.*, 2011). The penetrated synergid degenerates and the remaining one stays intact until a process of programme cell death is triggered (Higashiyama *et al.*, 2001; Dresselhaus and

Franklin-Tong, 2013).

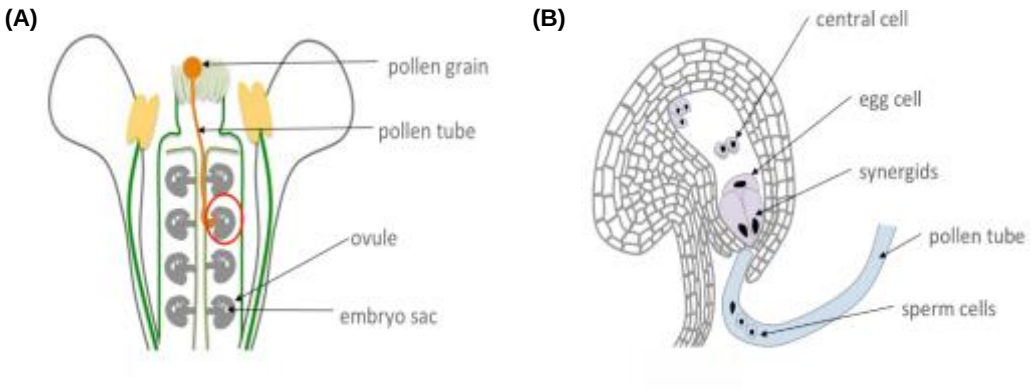

Figure 1. Schematic representation of the pollen tube growth through the pistil until it reaches the embryo sac in *Arabidopsis thaliana*. **(A)** The figure illustrates a pollen grain landing on the stigma and germinating into a pollen tube. The pollen tube grows along the style and the transmitting tract. **(B)** Once near an ovule, the direction of the pollen tube growth turns to the ovule entrance, where it will penetrate a synergid and release the sperm cells. (Adapted from Pereira *et al.*, 2014).

1.1.1. Ovule and megagametophyte: a synchronized development

A correct development of the ovule is required since inside of it, crucial events for sexual plant reproduction take place, such as the formation of the megagametophyte, followed by double fertilization, embryogenesis and finally, seed formation. The wild type (WT) ovule arises as a small fingertip-like structure from regions localized on the internal surface of the carpels. At this stage, the ovule primordium can be distinguished into three zones: the nucellus [where a megaspore mother cell will give rise by meiosis to the haploid megaspores], the chalaza [a central region where integuments formation occurs] and the funiculus [a supporting stalk which connects the ovule to the carpel's placenta]. The nucellus provides a source for megasporocyte differentiation, where the megaspore mother cell (MMC) develops, without any cell division. Still during this stage, the two integuments (inner and outer) initiate their development. These sporophytic tissues will result in thick layers of cells, which will enclose the nucellus and protect the haploid generation during ovule development (Figure 2A). After MMC meiosis and spore tetrad formation, megasporogenesis ends and only one of the four megaspores, the functional megaspore, enters megagametogenesis (the other three spores will degenerate) (Figure 2B). After three rounds of mitosis and differentiation, the embryo sac is completed. In *Arabidopsis*, the female gametophyte exhibits a *Polygonum*-type pattern (reviewed by

Maheshwari, 1950) composed by two synergid cells (cells responsible for pollen tube attraction, where pollen tube enters, burst and releases its gametes), the central cell (with two polar nucleus) and egg cell (the female gametes) and three antipodals (accessory cells that eventually will degenerate) (Schneitz *et al*., 1995).

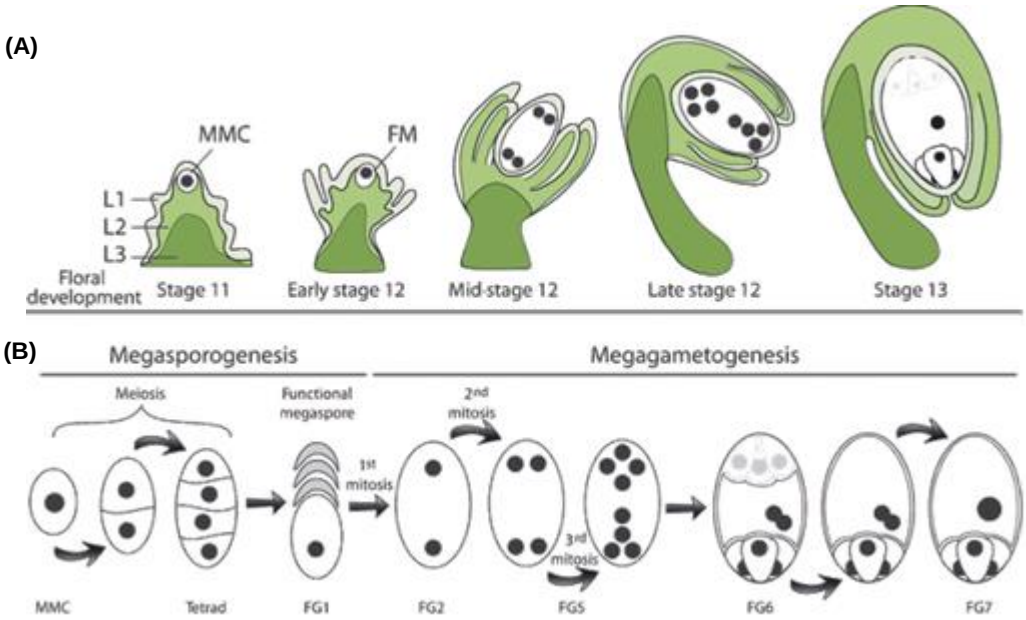

Figure 2. Ovule and female gametophyte development are synchronized in *A. thaliana*. **(A)** Integument initiation occurs in parallel with megasporogenesis (stage 11). As megagametogenesis continues, the integuments elongate (Early Stage 12). The integuments grow upward around the nucellus (mid-stage 12); and as the embryo sac is maturing (late stage 12), the outer integument begins to cover both the inner integument and the nucellus (floral development stages are according to Smyth *et al.*, 1990). At maturity, the outer integument delimits the micropyle, which is close to the funiculus. FM, functional megaspore. **(B)** Megasporogenesis and megagametogenesis in *Arabidopsis*. A megaspore mother cell (MMC) undergoes two successive meiosis to form a tetrad, of which three cells degenerate. The remaining FM undergoes three successive rounds of mitosis within a syncytium, followed by nucleus positioning and cell differentiation. The mature embryo sac has two synergids, one egg cell and one central cell. FG1-7, female gametophyte stage 1–7, according to Christensen *et al.* (1997). (Adapted from Chevalier *et al.*, 2011).

1.1.2. Seed development in *A. thaliana*

After fertilization of the egg and central cell, the development of a seed is initiated, resulting in a seed that can be divided into three different regions: embryo, endosperm and seed coat (SC) (Figure 3A) (for review see Nowack *et al.*, 2010). The embryo goes through stereotypic cell-division patterns, which culminate in the embryo proper (the body of the vegetative plant) and the suspensor (an ephemeral structure that allows

communication between the embryo proper and the SC) (Belmonte *et al.*, 2013; Lafon-Placette and Köhler, 2014). The endosperm, a nourishing tissue that supports embryo growth and germination, undergoes nuclei divisions and the nuclei migrate to form three subregions: micropylar, near the young embryo; peripheral, in the centre of the endosperm region; and chalazal, at the opposite pole of the embryo (Brown *et al.*, 1999; Lafon-Placette and Köhler, 2014). The SC derives from the maternal integuments, which show a rapid growth upon fertilization (Moïse *et al.*, 2005; Ezquer *et al.*, 2016). The distinct cell types of the SC surround the embryo and endosperm, protecting them from external factors such as UV radiation or pathogens (Haughn and Chaudhury, 2005). Furthermore, the SC is involved in transferring nutrients from the maternal plant to the embryo and endosperm, and functions as a barrier to precocious germination (Becker *et al*, 2014). These morphological alterations represent the morphogenesis phase of seed development. The maturation phase is characterized by an accumulation of macromolecules that help protecting the embryo and preparing it for desiccation. Once the seed is mature, it must separate from the plant in a process called seed abscission (Lewis *et al.*, 2006; Balanzà *et al.*, 2016). It requires a seed abscission zone (SAZ) composed of: a separation layer, with thin cell walls near the seed body, that will degenerate at the end of the process and an adjacent layer with lignified cells (lignified layer), which will produce the tension necessary for the separation of the seed from the funiculus (Figure 3B).

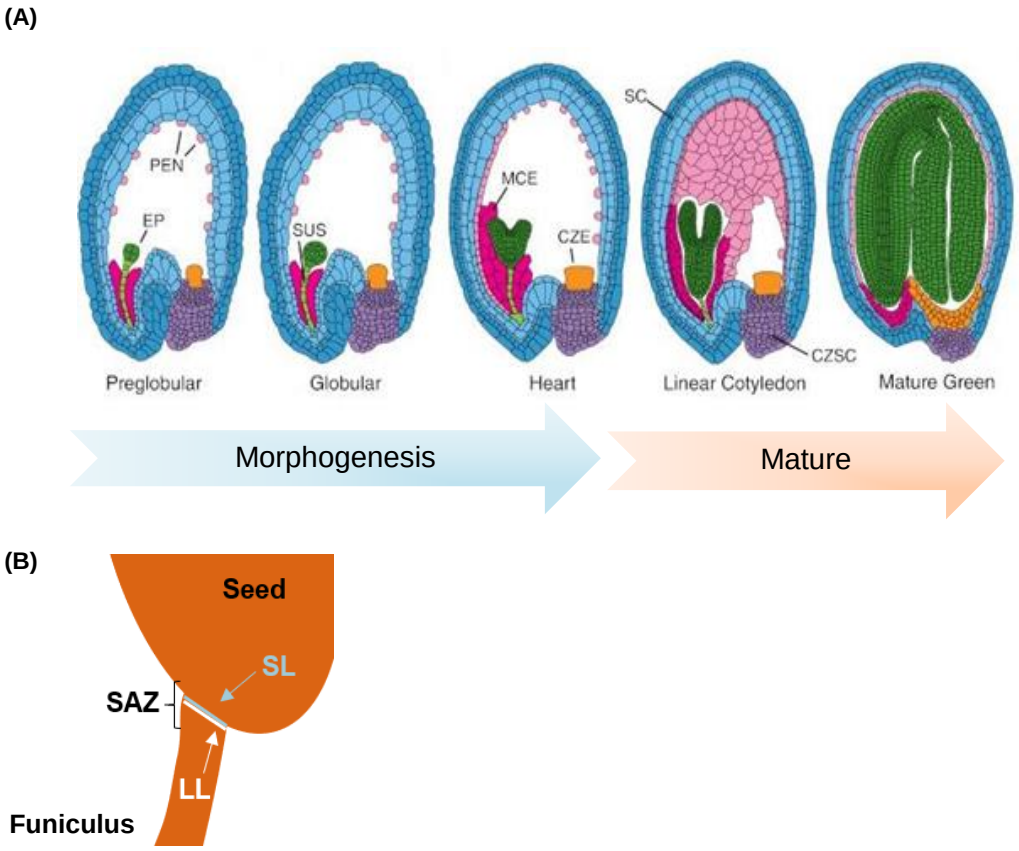

Figure 3. Schematic representation of *A. thaliana* seed development. **(A)** Representation of seed subregions in *Arabidopsis* from the preglobular to mature green stages of development. Green, embryo proper (EP); dark pink, micropylar endosperm (MCE); light pink, peripheral endosperm (PEN); orange, chalazal endosperm (CZE); purple, chalazal seed coat (CZSC); blue, seed coat (SC). (Adapted from Becker *et al.*, 2014*)*. **(B)** Representation of the seed abscission zone in *A. thaliana* seed. LL - lignification layer; SL - separation layer; SAZ - seed abscission zone. (Adapted from Balanzà *et al.*, 2016).

1.1.3. SEEDSTICK: a regulator of ovule development

SEEDSTICK (STK) is a transcription factor (TF) belonging to the MADS-box family and essential for a viable seed formation. Generally, the MADS TFs regulate the transcription process by forming tetramers: one TF dimerizes with another to form a homo or heterodimer and then, the two dimers form a heterotetramer. The MADS-domain TFs that composed the quartet will bind to two nearby CArG box, which are the DNA-binding site of the MADS proteins, in the target promoter. This will cause a loop in the DNA (reviewed by Yan *et al.*, 2016).

By using a SEEDSTICK-green fluorescent protein (GFP) reporter line, Mizzotti *et al*. (2014) were able to demonstrate the expression pattern of STK. At the beginning of ovule development, STK was detected in the placental tissues and along the ovule primordia (Figure 4A). Later, as the inner and outer integuments start to develop, the GFP signal appears only in the nucellus and funiculus (Figure 4B). At the subsequent stages until a mature seed is formed, STK continues to be expressed in the growing funiculus and its signal detection extends to the outer integument and outer layer of the inner integument (Figure 4C-E).

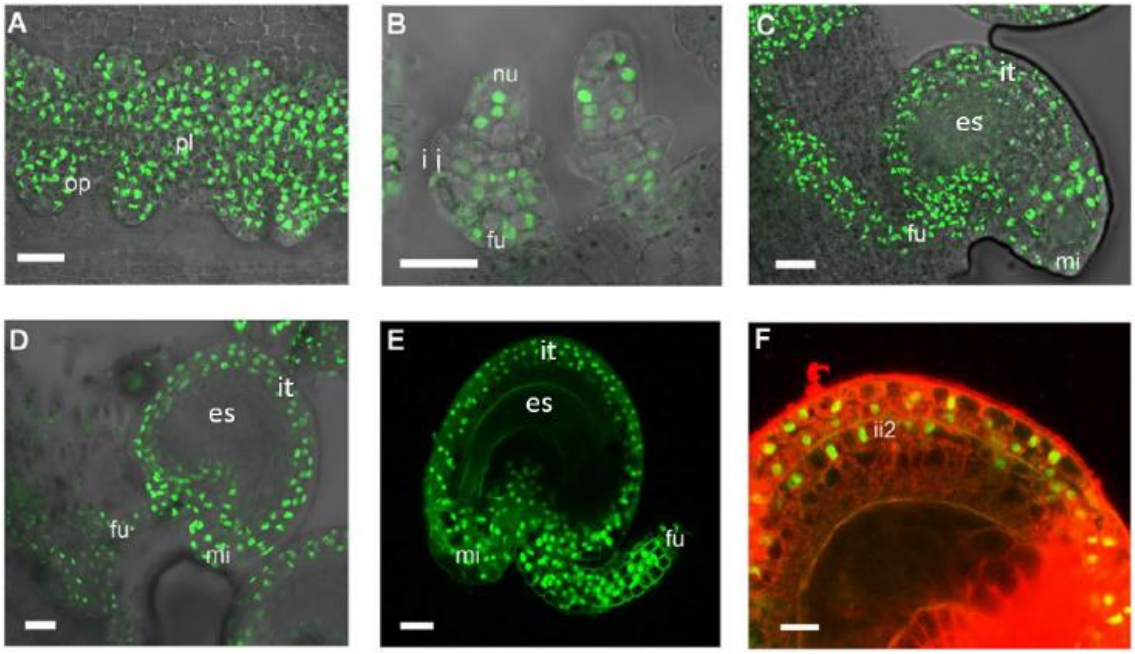

Figure 4. Confocal laser-scanning images of *pSTK:STK-GFP* expression patterns during ovule and seed development. **(A)** STK-GFP protein is expressed in the placenta and in the ovule primordia. **(B)** When integuments arise, STK-GFP signal is localized in the nucellus and in the funiculus. **(C, D)** when the ovule is mature**,** GFP signal can be detected throughout the integuments, funiculus and the adjacent placental region. **(E)** After fertilization, the STK-GFP signal is present in the outer integuments and funiculus of developing seeds. **(F)** Magnification of figure E with an overlay image of propidium iodide staining (specific staining of the cell wall). STK-GFP can be detected in the two layers of the outer integument and in the outer layer of the inner integument. fu - funiculus; it - integuments; ii2 - outer layer of inner integument; mi - micropyle; nu - nucellus; op - ovule primordia; pl – placenta. Scale bars = 50 µm (A and B), 40 µm (C, D and E) and 20 µm (F). (Adapted from Mizzotti *et al*., 2014).

This expression pattern together with many genetic-based studies performed over the years supports the involvement of STK in ovule development until seed formation. STK is a powerful ovule-identity TF capable of converting WT sepals into carpeloid organs containing ovule-like structures, when overexpressed in *A. thaliana* plants (Favaro *et al.*,

2003). It redundantly controls ovule identity together with SHATTERPROOF1 (SHP1) and SHP2. In the *stk shp1 shp2* triple mutant, ovules are converted into carpel-like or leaf-like structures, while single or double mutant combinations of these genes do not affect ovule identity (Pinyopich *et al.*, 2003). The phenotype analysis of *bell1 (bel1) stk shp1 shp2* quadruple mutant, plus the results from yeast-three-hybrid and pull-down assays, revealed that an ovule identity complex, which STK is part of, regulates the outer integument development by stabilizing the complex BEL1-AGAMOUS-SEPALLATA3. Then, this complex will activate the expression of *INNER NO OUTER* (*INO*) (Baker *et al*., 1997), a gene needed for the outer integument outgrowth (Brambilla *et al*., 2007, 2008; Battaglia *et al*., 2008). As mentioned before, STK is also involved in seed formation. *stk* seeds were smaller compared to the WT ones and the funiculus was thicker and longer, at floral stage 17 according to Smyth *et al.* (1990). Furthermore, the mutant displayed defects in the SAZ that resulted in a lack of seed dispersion (Pinyopich *et al.*, 2003). Recently, a model was proposed in which STK would act as a repressor of lignin deposition in the SAZ, enabling seed detachment (Balanzà *et al.*, 2016). Together with *Arabidopsis B Sister* (*ABS*), *STK* regulates endothelium formation, the innermost layer of the inner integument. The *abs* mutant develops a deformed endothelium with flatter cells (Nesi *et al*., 2002). However, the *abs stk* double mutant has no endothelium, which led to a severely reduced seed set (Mizzotti *et al.*, 2012).

1.1.4. Funiculus: an umbilical-cord-like structure

The funiculus is a structure that stays intact throughout ovule development until seed dehiscence, allowing the connection between the maternal plant and the ovule/seed, which highlights the importance of its biological function. Curiously, not many studies regarding morphological and histological analysis of *A. thaliana* funiculi are available, even though these subjects are extensively studied in other plants like *Brassica napus* (Chan and Belmonte, 2013) or *Phaseolus vulgaris* (Mawson *et al.*, 1994). Light micrographs of the funiculus showed that this tissue is composed of an outer epidermis, a parenchymatous cortex, and an internal vascular core with xylem and phloem (Figure 5). Cells of epidermis and cortex are similar in size, while the ones of the vasculature are smaller. Additionally, by using an electron microscope, Khan *et al.* (2015) presented evidence of an endomembrane system and observed numerous plasmodesmata between the funiculus cell layers. Finally, it was demonstrated that the funiculus

vasculature proliferates and consequently, the epidermis and cortex cells also proliferate through anticlinal divisions.

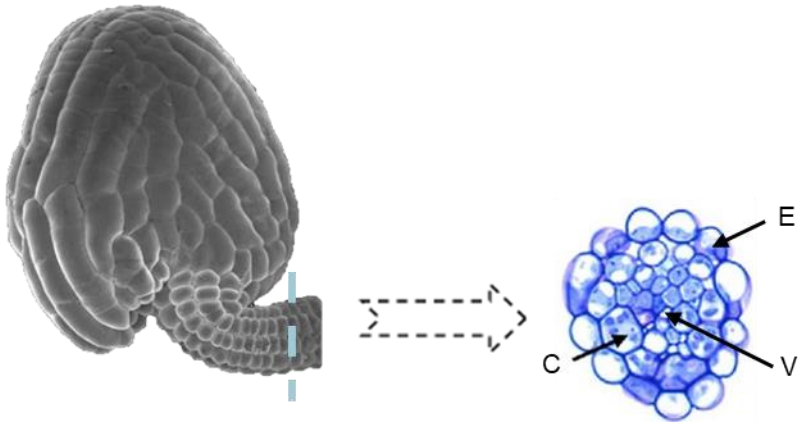

Figure 5. Schematic representation of the funiculus morphology. Cross-section of a funiculus showing the epidermis (E), cortex (C), and vasculature (V). (Adapted from Khan *et al*., 2015).

Until now, only two genes were identified as being involved on funiculus development. *STK* participates on funiculus cell division and proliferation and defines a SAZ on mature funiculus (Pinyopich *et al.*, 2003; Balanzà *et al.*, 2016). On the other hand, *SPOROCYTLESS/NOZZLE* indirectly controls funiculus growth by defining the chalaza and integuments identity (Balasubramanian and Schneitz, 2000). The analysis of these mutants shows that alterations on the funiculus culminate on seed deformations. However, the network involved in these modifications has not yet been revealed.

Recently, a transcriptomic analysis of funiculi was performed using a microdissection laser and the genetic profiles were compared to the ones of zygotic regions and subregions, during seed development (Khan *et al.*, 2015). The results displayed the funiculus as a direct way for transportation of nutrients, minerals, sugars and maternal signals for the developing embryo and seed. For example, *K+ ATPase 1* and *REQUIRES HIGH BORON 1* messenger RNAs (mRNAs) were found to be funiculus specific. The accumulation of these transcripts related to transport increased along funiculus development. Moreover, the involvement of the funiculus in biological processes such as the glucosinolate metabolism and auxin response was predicted. Later, Larsson *et al.* (2017) confirmed the involvement of the funiculus in auxin response since it was found

that auxin biosynthesis genes and auxin transport proteins define a pre-patterning of vascular cell identity in the pre-anthesis funiculus.

1.1.5. Sporophyte and Megagametophyte: a cross talk during ovule development

As explained before, in seed plant ovules, the maternal sporophytic tissues embed and support the haploid generation, therefore two different generations coexist in the same organ. An interaction between these two has been proposed based on the analysis of sporophytic ovule mutants and it seems to be necessary for a correct seed development. When there is a defect in the embryo's sac surrounding tissues, megagametogenesis is severely impaired (for review see Bencivenga *et al.*, 2011). For example, in *stk shp1 shp2* ovules, integuments developed into carpel-like structures and the embryo sac maturation was arrested after megasporogenesis (Brambilla *et al*., 2007; Battaglia *et al*., 2008). In *bel1* ovules, an aberrant structure with carpel identity appears, instead of the integuments (Robinson-Beers *et al*., 1992) and the embryo sac is unable to develop since megagametogenesis stops at female gametophyte stage 1 (FG1). According to Christensen *et al.* (1997) (Figure 2B) *ino* mutants have a normal inner integument, but the absence of the outer integument resulted in megagametogenesis disorders (Villanueva *et al.*, 1999). The complete lack of endothelium in the *abs stk* ovules caused an extreme reduction in seed set (Mizzotti *et al*., 2012). It is worth noting that none of the genes stated above are expressed in the haploid lineage (Reiser *et al*., 1995; Villanueva *et al*., 1999; Mizzotti *et al*., 2014; Ehlers *et al*., 2016). Hence, two important questions arise: how is cell-to-cell signalling coordinated in ovule development and what is the nature of the players?

The correlation between hormones and ovule formation has been investigated and the analysis performed support the importance of hormones for the correct development of the ovule. *CTR1* (*CONSTITUTIVE TRIPLE RESPONSE 1*) gene is related to ethylene signal transduction and encodes a Raf-like Ser/Thr protein kinase (Kieber *et al.*, 1993). *ctr1* mutants show embryo sac defects that affect segregation ratios (Kieber and Ecker 1994; Drews *et al.*, 1998). Regarding auxin, *TRYPTOPHAN AMINOTRANSFERASE OF ARABIDOPSIS 1* (*TAA1*) expression is highly reduced in *aintegumenta* ovules, where integuments are severally affected, and the embryo sac is blocked at FG1 stage (Baker *et al.*, 1997; Nole-Wilson *et al.*, 2010). TAA1 is a tryptophan aminotransferase critical for

the synthesis of auxin (Stepanova *et al.*, 2008; Tao *et al.*, 2008), thereby demonstrating a sporophytic-megagametophytic dialogue via auxin biosynthesis.
Nevertheless, these hormone studies require a deep analysis and it is still possible that another type of messengers, such as peptides, ligands or small RNAs, might also be involved in the cross talk between the two ovule generations.

1.1.6. Peptide Signalling: a way of communication in reproduction

Emerging evidence clarified that peptide signalling is essential for plant development (Bedinger *et al.*, 2010; Kumpf *et al.*, 2013; Breiden and Simon, 2016), and reproduction is not an exception. Commonly, peptides that act as signalling molecules are released through the classical secretory pathway and diffuse to the neighbour cells over short distances to bind to its receptor. Over the years, different peptides and receptors have been identified as important molecules involved in pollen-pistil interactions, including gametophyte interactions (Figure 6) (for review see Higashiyama and Yang, 2017). These include determinants of self-incompatibility, factors for pollen germination and tube growth, and pollen tube attractants. Many of the identified peptides are considered cysteine-rich peptides (CRPs). This family of peptides includes gene classes encoding for defensin-like (DEFL) peptides, lipid-transfer proteins (LTP), early culture abundant 1 (ECA1) gametogenesis-associated peptides, rapid alkalinization factors (RALFs), among others. LURE peptides (Okuda *et al.*, 2009; Kanaoka *et al.*, 2011; Takeuchi and Higashiyama, 2012) belong to the DEFL class and were first discovered in *Torenia fournieri* (a fascinating plant species with a protruding embryo sac that has been used as a model plant for PT guidance studies). LURE1 peptides from *Arabidopsis* are secreted by the synergid cells and diffuse along the pathway of the PT until the surface of the septum, via the surface of the funiculus (Takeuchi and Higashiyama, 2012). The interaction with the PT is only accomplished due to the existence of tip-localized receptor-like kinases (RLK) (MDIS1-MIK [Wang *et al.*, 2016] and PRK3-PRK6 [Takeuchi and Higashiyama, 2016]), which sense LURE1 attractant peptides. Only recently it was demonstrated the involvement of RALFs with reproductive processes. RALFs are ubiquitous in the plant kingdom and known to be involved in physiological and developmental processes in *Arabidopsis* (Murphy and Smet, 2014). They are ligands for receptors of the *Catharanthus roseus* RLK1-like family, which are associated not only with cell expansion regulation (Bai *et al.*, 2014; Li *et al.*, 2016) but also with functions in

pollen tube reception at the point of contact with the female gametophyte (Escobar-Restrepo *et al.*, 2007; Miyazaki *et al.*, 2009). Indeed, it was discovered that RALF4 and RALF19 (two PT expressed peptide ligands) (Mecchia *et al.*, 2017) bind to the set of receptors ANXUR/BUPS, which are also localized in the PT. This interaction is in competition with RALF34 (a female derived ligand) at the interface of PT–female gametophyte contact. RALF34, then, replaces RALF4 and RALF19, allowing the rupture of PT and consequently, sperm release (Ge *et al.*, 2017).

Despite the fact that no peptide-receptor pairs have been reported for ovule's sporophytic tissues during ovule and/or seed development, recent studies suggest that the maternal sporophytic tissues might release small molecules as signals during important processes for reproduction. For example, the funiculus is a plausible tissue that emits a repellent (maybe a CRP), which blocks polytubey (Shimizu and Okada, 2000). The paths on the funiculus of WT pistils for PT orientation are divided into two phases: funicular guidance and micropyle guidance (Higashiyama *et al.*, 2003). The first one would guide a PT from the transmitting tissue onto the surface of a funiculus. Then, another guidance signal, the micropyle guidance signal, would lead the PT to the micropyle. *mitogen-activated protein kinase 3* (*mpk3) mpk6* mutant pollen tubes were defective in the funicular guidance phase, while no alterations were observed during the micropylar phase (Guan *et al.*, 2014). This suggests the existence of ligands in the funiculus tissue that will bind to receptors such as MPK3 and MPK6 present in the PT, allowing its orientation. Funicular guidance cues were reported to be governed by the female gametophyte (Shimizu and Okada, 2000). Recently, data revealed on the 25th International Congress on Sexual Plant Reproduction corroborates this idea. In a poster titled "Analysis molecular mechanism of *FG1* in regulating pollen tube guidance and funiculus development", presented by Hui Zhou (Institute of Genetics and Developmental Biology, Chinese Academy of Sciences), a TF (FG1), specifically expressed in the funiculus, was shown to be down regulated on the c*entral cell guidance mutant* (*ccg*)*. CCG* is a gene expressed in the central cell, which encodes for a TF (Chen *et al.*, 2007). The analysis of *fg1* mutant displayed defects in funicular guidance with addition of a high rate of unfertilized ovules. The fact that CCG might be controlling the expression of *FG1* supports the idea of funicular guidance cues coming from the megagametophyte. However, it can also be indirectly derived from sporophytic tissues such as the integuments (Higashiyama, 2010). *ino* mutants display a disruption in PT guidance

(Baker *et al*., 1997), indicating that the outer integument might be involved in this process too.

Regarding post-fertilization events, a SAZ is formed in the funiculus, allowing seed abscission. STK is a key factor for the establishment of the lignin pattern in the SAZ. This TF interacts with SEUSS co-repressor, and together they function as repressors of *HECATE3*, enabling a correct deposition of lignin in the vasculature of funiculus cells (Balanzà *et al.*, 2016). Remarkably, this study only reported transcription factors acting downstream of STK network. Floral abscission in *Arabidopsis* is a similar process to seed abscission. It was reported that floral abscission is regulated by peptide signalling (Aalen *et al.*, 2013; Meng *et al.*, 2016), consisting of a peptide ligand, INFLORESCENCE DEFICIENT IN ABSCISSION, its RLKs, HAESA and HAESA-LIKE2, and a downstream MPK cascade. Therefore, it is reasonable to hypothesize that a ligand-receptor pair may also play a role in the correct formation of the SAZ.

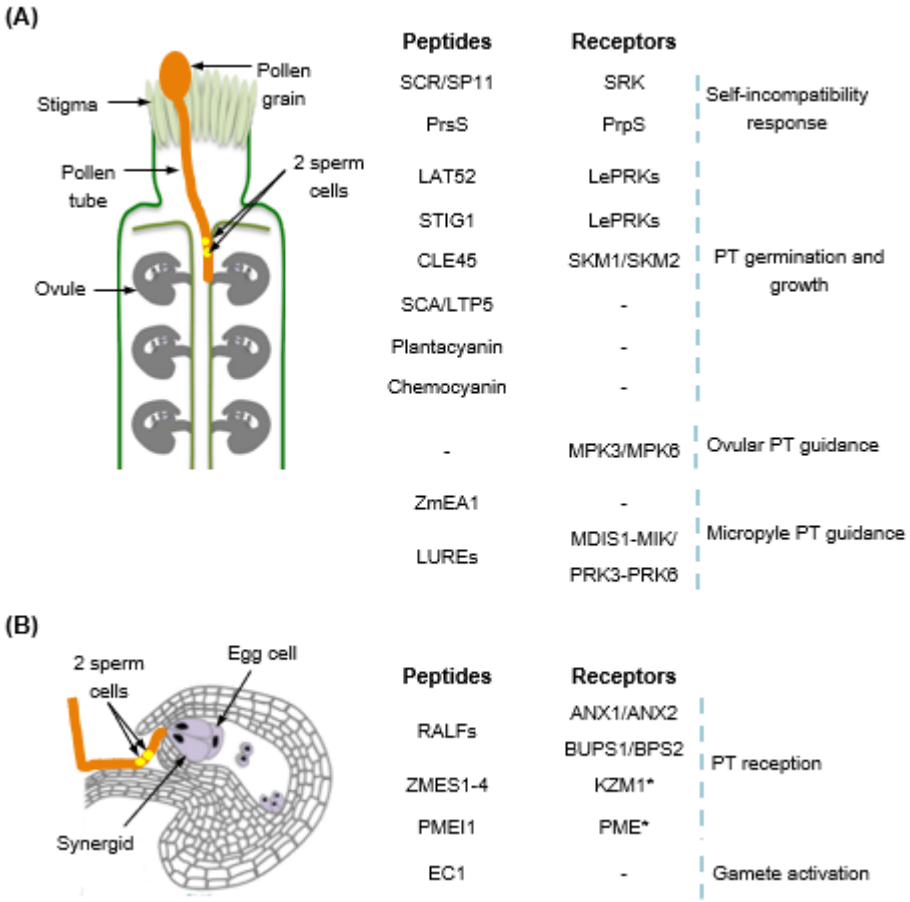

Figure 6. Schematic representation of secreted peptides and their receptors involved in pre-zygotic communication of reproductive cells**. (A)** Pollen-pistil interactions in self-incompatibility responses, pollen tube growth and guidance. Ovular guidance is mediated by signals derived from sporophytic ovule tissues while micropylar guidance is mediated by signals from female gametophytic cells. **(B)** Enlarged image of an ovule right before sperm cell release is shown. The role of peptides and receptors is detailed in the text. Please note that peptide targets including ion channels such as KZM1 and enzymes such as PME (indicated by one asterisk) are not receptors in the 'classical' sense. (Adapted from Qu *et al.*, 2015).

1.2. Objectives

By 2050, the world's population will reach 10 billion people, which means that a solution to feed this growing population has to be found (FAO, 2017). It will be necessary to increase agricultural yields without using more arable land and water. The core purpose of agriculture is to produce viable seeds since they account for the majority of calories consumed by humans, are significant components of animal feed and are a major source for the production of high-value-added products. Hence, understanding the factors involved in seed production will help in obtaining plants with higher yields. The work presented hereby is included in the SEXSEED project, created to improve our knowledge on seed formation in model plants species and then transfer this data horizontally into agricultural crop species with economic value. Furthermore, this consortium, which is funded by the EU Horizon 2020 Research and Innovation Staff Exchange programme, aims to provide new insights into the role and the network of genes controlled by SEEDSTICK (STK), a transcription factor critical for plant reproduction and for a successful seed formation.

The analysis of ovule's sporophytic mutant tissues clearly point to a cross talk between the sporophyte and megagametophyte. However, how this communication occur is still unknown. It might be accomplished by peptide signalling, where a peptide ligand binds to a specific receptor, originating a cascade of events. Currently, there is a gap regarding the peptide and receptors pairs present in the sporophytic ovule tissues, namely the funiculus and integuments. Since *STK* is highly expressed in these tissues, a bioinformatic analysis on the *stk* RNA-seq data was done with the purpose of inquire if peptide signalling related genes expression was being controlled by STK. The second aim was to identified ligand-receptor pairs present in the integuments and/or in the funiculus. Therefore, STK reporter line and *stk* mutant line were used to obtain a transcriptome from these sporophytic tissues during two different stages: before and after fertilization. To finalize, it was important to address STK involvement during PT guidance and regarding the development of the funiculus because they are processes which occur during the stages and involving the tissues selected for the transcriptome. Furthermore, the phenotypes in the *stk* mutant are not completely elucidative. Hence, accurate techniques were performed. This multifaceted work purposed here will shed lights on STK regulatory network.

2. Materials and Methods

2.1. Bioinformatics analysis

The Differentially Expressed Genes (DEG) of *stk* inflorescences transcriptomic data (Mizzotti *et al.*, 2014) was crossed with a list of CRPs under-predicted in plants (Silverstein *et al.*, 2007), which was named as CRPs_Silverstein, and a list of CRPs found in *A. thaliana* WT ovules (Huang *et al.*, 2015), represented as CRPs_Huang. A threshold of a False Discovery Rate (FDR) < 0.05 was defined and the selected genes were briefly described using TAIR (https://www.arabidopsis.org/). The predicted expression pattern was based on e-FP Browser tool (http://bar.utoronto.ca/efp/cgi-bin/efpWeb.cgi), Klepikova Arabidopsis Atlas e-FP Browser (Klepikova *et al.*, 2016) and the expression pattern defined by Huang *et al.* (2015).

2.2. Plant material and growth conditions

For all experiments, accession Columbia (Col-0) was used as a wild type *A. thaliana*. WT seeds were obtained from the Nottingham Arabidopsis Stock Center (NASC), United Kingdom. *stk-2* (Pinyopich *et al.*, 2003) mutant line and *pSTK:STK-GFP* (Mizzotti *et al.*, 2014) reporter line were kindly provide by Lucia Colombo Lab, Universitá degli Studi di Milano. The *stk-2* allele contains a 74 nucleotide insertion near the splice site of the third intron. In all the experiments, flowers utilized were from either stage 12 or 17 (according to Smyth *et al.*, 1990). Stage 12 flowers used had the sepals opened, allowing to see a small portion of the petals. Stage 17 siliques used in the studies were defined as the first three siliques counting from the top to the base of the stem, starting on the younger silique, whose floral parts fell.

Seeds were surface sterilized in the laminar flow hood, using a bleach solution. Less than 100 µL of each seeds line were placed in 1.5 mL eppendorf tubes, where it was added 1 mL of 1% NaClO/ 0.02% Tween-20 solution. The tubes were shaken for 3 minutes to soak the seeds and then, a washing step with ddH_2O was performed and repeated 3 times. 1 mL of 0.1% Plant preservative mixture/0.02% Tween-20 solution was added to each tube and they were placed in the dark for 1-2 days at 4ºC, in order to break the seeds dormancy. Afterwards, the supernatant was removed, 0.1% agar was added to the tubes and, using a tip, the seeds were transferred to 1/2 MS (Murashige

and Skoog) media plates, containing 1% (w/v) sucrose (pH 5.8 with KOH) solidified with 0.8% (w/v) agar. The plated seeds were placed in a growth chamber at 22ºC and continuous light. When seedlings were 7 to 10 days old, they were moved to soil pots and were grown in a growth chamber under long-day conditions: 16 hours light at 21ºC and 8 hours dark at 18ºC.

2.2.1. Preparation of plant material for microscopy

To check the fluorescence of *pSTK:STK-GFP* line, under a SZ61 stereo microscope (Olympus) and using hypodermic needles, pistils were removed from the flowers, dissected and ovules were mounted in a microscope slide with H_2O. Then, observation of the ovules occurred using an inverted microscope (IX71, Olympus) equipped with GFP channel. Images were captured with a 3CCD camera (C7780-20, Hamamatsu Photonics), using the cellSens software.

Pistils and siliques from WT and *stk* plants from both stages 12 and 17 (Figure 14) were collected and placed on a microscope slide, under the SZX16 stereo microscope (Olympus). Images were captured using the U-CMAD3 camera (Olympus).

Pictures from Figure 11 were captured while the procedure was being done, using a SZX16 stereo microscope (Olympus) equipped with a U-CMAD3 camera (Olympus).

2.3. Genotyping

stk mutant line was confirmed by Polymerase Chain Reaction (PCR). A small leaf disk was enough to extract the amount of genomic DNA (gDNA) required for PCR amplification. The gDNA was extracted according to Edwards *et al.* (1991). The PCR was carried out using GoTaq® Green Master Mix (Promega). Specific primer sequences and expected band sizes are listed in Supplemental Table 1 and PCR mixture is represented on Table 1.

Table 1. Reaction mixture used for PCR.

Reagent	Concentration
2x GoTaq Green Master Mix	1x
Primers	10 mM
Template	0 pg- 1 µg
Nuclease-free H_2O	up to 10.0 µL

A PCR Thermal Cycler Dice® Gradient (TaKaRa) was used and the program was set according to Table 2.

Table 2. PCR conditions used for genotyping.

Step		Temperature	Time
Initial denaturation		95ºC	2 min
35 Cycles	Denaturation	95ºC	30 sec
	Annealing	60ºC	50 sec
	Extension	72ºC	1 min
Final extension		72ºC	5 min

PCR products were separated in a 2% (w/v) agarose gel in 1X TAE (40 mM Tris-acetate and 1 mM EDTA, pH 8.3); 0.5 mg/mL ethidium bromide was added prior to polymerisation. Using the Gene Ladder 100 (Nippon Gene) as a molecular weight marker and 1X TAE as running buffer, the electrophoretic separation was conducted at 100 V and non-limiting amperage for 30 minutes. The DNA was visualized in a UV transilluminator (302-365 nm).

2.4. Protoplast isolation

Emasculated pistils from stage 12 were dissected under a SZ61 stereo microscope (Olympus), using hypodermic needles. Ovules from one pistil were released to a plastic disk containing 100 µL of enzymatic solution, and the disk was placed at 28ºC with different incubation times. Three enzymatic solutions were used. Solution 1 was as described by Kawano *et al.* (2011) with some modifications: 1% cellulase (CEL, Worthington), 0.3% maceroenzyme (R-10, Yakult), 0.05% pectolyase (Y-23, Yakult) and 0.45 M mannitol. Solution 2 had the same composition as solution 1 with the only difference being the addition of two enzymatic enhancers: 1 mM $CaCl_2$ and 0.2% BSA (Bovine Serum Albumin). Solution 3 was as described by Park *et al.* (2016) and consisted of 1% cellulose (CEL, Worthington), 0.5% maceroenzyme (R-10, Yakult), 0.1% pectolyase (Y-23, Yakult), 0.4 M mannitol, 10 mM $CaCl_2$, 0.1% BSA, 20 mM KCl and 20 mM MES (4-morpholineethanesulfonic acid), pH 5.7. Before the addition of enzymes and $CaCl_2$, the MES solution containing mannitol and KCl was preheated at 70ºC for 5 minutes to resolubilize any crystals. The solution was then allowed to cool to room temperature, and enzymes were added, followed by incubation of the solution at 55ºC for 10 minutes, enhancing enzyme solubility. 10 mM $CaCl_2$ was added after the solution reached room temperature. The final enzyme solution was filter sterilized by syringing through a 0.45 µm membrane. Protoplasts were observed in bright field under an inverted microscope (IX71, Olympus) and pictures were taken with a 3CCD camera (C7780-20, Hamamatsu Photonics), using the cellSens software.

2.5. Nuclei isolation

Nuclei isolation procedure from WT and *ATML1::NLS-VENUS* leaves was adapted from Deal and Henikoff (2011) and performed as follows: 0.1 g of leaves were grinded in liquid N_2 and the powder was resuspended in 5 mL of cold nuclei purification buffer (NPB) [20 mM MOPS, pH 7; 40 mM NaCl; 90 mM KCl; 2 mM EDTA; 0.5 mM EGTA, pH 8; 0.5 mM spermidine]. Afterwards, the extracts were filtered to a 50 mL falcon tube through a 70 µm nylon mesh and they were centrifuged at 1000 rpm for 3 minutes. The nuclei were gently resuspended in 500 mL of cold NPB and moved to a 1.5 mL eppendorf tube. Cell sorting of *ATML1::NLS-VENUS* leaves nuclei solution was performed using the SH800 cell sorter (Sony, Tokyo, Japan).

The isolation of nuclei from *pSTK:STK-GFP* line was performed according to DW-K *et al.* (2012) with some modifications. Ten pistils per sample were emasculated, and 24 hours later, they were dissected under a SZ61 stereo microscope (Olympus), using hypodermic needles. Ovules were placed inside of an eppendorf tube, containing 20 µL of nuclei isolation buffer (NIB) [0.25 M sucrose; 15 mM Piperazine-N, N′-bis (2-ethane-sulfonic acid), pH 6.8; 5 mM $MgCl_2$; 60 mM KCl; 15 mM NaCl; 1 mM $CaCl_2$; 0.9% Triton X-100; 1 mM PMSF (phenylmethanesulfonyl fluoride)]. With a pre-cooled pestle, the ovules were macerated and 300 µL of NIB was added. The samples were incubated on ice for 15–30 minutes, subjected to centrifugation at 1000 g for 4 minutes at 4ºC, ressuspended and filtered through a 0.45 µm membrane. All the steps were performed on ice whenever possible. For the isolation of nuclei from pre-fixed ovules, ovules were obtained in the same way as described above, but they were first placed in 50 µL of RNAlater™ Stabilization Solution (Ambion) and 4% paraformaldehyde solution was added. After 5 minutes incubation at room temperature, the samples were macerated with a pestle and centrifuged at 1500 g at 4ºC for 1 minute. Supernatant was removed for the solution become 2x concentrated, 100 µL of NIB was added and the tubes were placed on ice for 15 minutes. The samples were centrifuged, and supernatant was removed. Finally, samples were filtered through a 0.45 µm membrane.

To each sample analysed under the microscope, 5 µM of 4′,6-diamidino-2-phenylindole (DAPI) was added. The nuclei samples were analysed with an Axio Imager A2 microscope (Zeiss) equipped with a DAPI and a GFP channel. Images were captured with an Axiocam 506 color (Zeiss), using Zen 2 software (Zeiss).

2.6. Transcriptome from funiculus cells

2.6.1. Collection of funiculi and ovules from *A. thaliana*

Under a SZ61 stereo microscope (Olympus), WT and *stk* pistils from both stages 12 and 17 flowers were first dissected, and ovules were placed into a 50 µL droplet of medium (whose composition had been described in Gooh *et al.*, 2015) in a plastic dish (Φ 3.5 cm). Each funiculus was separated, using a surgical knife and, one at a time, they were transferred with a tungsten needle to another plastic dish, containing 10 µL of medium. Then, each funiculus was transferred to an eppendorf, which already had 40 µL of RNAlater™ Stabilization Solution (Ambion). For samples containing only ovules, 5 pistils

were dissected in the same conditions as described before and all the ovules were transferred to the inside of an eppendorf tube with 40 µL of RNAlater™ Stabilization Solution (Ambion).

2.6.2. mRNA extraction and cDNA synthesis

mRNA was extracted from both WT and *stk* funiculi and ovules, from stages 12 and 17 flowers, using the Dynabeads™ mRNA DIRECTTM Micro Kit (Invitrogen) according to the manufacturer's instructions. RNA was retro-transcribed using the High-Capacity RNA-to-cDNA™ Kit (ThermoFisher). Reaction mixture was as described in Table 3.

Table 3. Reaction mixture used for RNA retro-transcription. RT – Reverse Transcriptase.

Component	Volume per reaction (µL)
2x RT Buffer Mix	10.0
20x RT Enzyme Mix	1.0
RNA sample	up to 9.0
Nuclease-free H_2O	Q.S. [1] to 20.0
Total per reaction	20.0

[1] Quantity Sufficient

The reaction was incubated at 37ºC for 60 minutes. Then, it was stopped by heating to 95ºC for 5 minutes. cDNA samples were kept at -30ºC.

2.6.3. Validation of mRNA and cDNA quality

mRNA quality from funiculi and ovules samples were validated using the Agilent RNA 6000 Pico Kit (Agilent Technologies), followed by a running of the chip in an Agilent 2100 Bioanalyzer (Agilent). cDNA was tested by a semiquantitative reverse transcriptase (RT)-PCR using *AGP9* (*AT2G14890*), *AGP4* (*AT5G10430*), *SUS4* (*AT3G43190*), *FIS2* (*AT2G35670*) and *ACT7* (*AT5G09810)* primers. Specific primer sequences and

expected band sizes are listed in Supplemental Table 1. PCR and electrophoretic separation were performed as described earlier.

2.6.4. RNA-sequencing library preparation

mRNA was extracted from one sample containing 100 funiculi from stage 12 of both WT and *stk*, from three biological replicates of 100 funiculi from stage 17 of both WT and *stk* and from another three biological replicates of ovules from 5 pistils at both stage 12 and 17 of WT and *stk*. Sequencing libraries were prepared according to the manufacturer's instructions, using the TruSeq® RNA Sample Preparation v2 (Illumina Inc.) and sequenced with a NextSeq 500 sequencer (Illumina). Sequencing and data analysis were performed as reported in Kadokura *et al.* (2018).

2.7. Aniline blue staining of pollen tubes

WT and *stk* pistils from stage 12 flowers were emasculated and 24 hours later, they were hand pollinated with WT pollen. 12 hours after, pistils were collected and fixed in absolute ethanol and glacial acetic acid in a 3:1 ratio and left for more than 2 hours at 4ºC. The material was washed in 70% ethanol, 50% ethanol, 30% ethanol, 10% ethanol and finally in ddH_2O, for 20 minutes each. After overnight incubation 1 M NaOH at 4ºC, the material was washed two times with ddH_2O and stained with 0.1% (w/v) decolorized aniline blue solution (DAB) (in 0.1 M K_3PO_4). The material was observed under an ultraviolet illumination using an upright Axio Imager A2 microscope (Zeiss). Images were captured with an Axiocam 506 color (Zeiss), using Zen 2 software (Zeiss).

2.8. SR2200 staining

SCRI Renaissance 2200 (SR2200) staining was performed as reported in Musielak *et al.* (2016). Briefly, WT ovules were manually dissected out of the pistil and collected in a drop of staining solution on a microscope slide. Soft vacuum was applied for 5 minutes at room temperature. Afterward, the staining solution was replaced by ddH_2O and again incubated under soft vacuum for 5 minutes. After replacing the water with 10% glycerol, the sample was mounted under a coverslip. Images were obtained with a LSM780NLO

confocal microscope (Zeiss) and processed with ZEN software (Zeiss). SR2200 was excited with a 405 nm laser line and emission recorded between 415 and 476 nm (405/415–476). Two pistils from different plants were used.

2.9. Propidium iodide staining

Propidium iodide (PI) staining was used to stain funiculi. For that, WT ovules from one pistil were collected, mounted in 10 µg/mL of propidium iodide in water, and analysed. A LSM780NLO confocal microscope (Zeiss) was used and images were processed with ZEN software (Zeiss). PI was excited with a 543 nm laser line and emissions were detected between 600 and 640 nm (543/600-640). For observations, ovules from 2 pistils were analysed.

2.10. CalcoFluor White M2R staining

Pistils previous emasculated and siliques were harvested and fixed in absolute ethanol and glacial acetic acid in a 3:1 ratio and left for more than 2 hours at 4ºC. The material was washed in 70% ethanol, 50% ethanol, 30% ethanol, 10% ethanol and finally in ddH_2O, for 20 minutes each. After incubation on 1 M NaOH at 4ºC for more than two days, the material was washed in ddH_2O for 30 minutes, stained with 1% Calcofluor White M2R, freshly made, for 1 hour and washed again in ddH_2O for another 30 minutes. After mounting the samples in water in a slide microscope, they were immediately observed. A LSM780NLO confocal microscope (Zeiss) equipped with a chameleon laser was used and images were processed with ZEN software (Zeiss). For confocal imaging, Calcofluor White M2R was excited with a. 405 nm laser line and emissions were detected between 425 and 475 nm (405/425-475), while for two-photon imaging, the excitation was in 900 nm and emissions were around 780 to 810 nm (900/780-810). The observations were done in two pistils and two siliques.

2.11. SyBr Green I staining

Pistils previous emasculated and siliques were collected and cleared in ClearSee solution following the protocol of Kurihara *et al.* (2015). After one-month incubation in ClearSee, the samples were stained in 0.1% Calcofluor White M2R (prepared in

ClearSee) for 1 hour and washed in ClearSee for 30 minutes. The samples were stained with SYBR™ Green I Nucleic Acid Gel Stain (Invitrogen) diluted 10 times in ClearSee for 30 minutes, washed 3 times for at least 30 minutes in ClearSee and mounted on slides with ClearSee solution for imaging. A LSM780NLO confocal microscope (Zeiss) was used and images were processed with ZEN software (Zeiss). Calcofluor White M2R was excited with a 405 nm laser line and emissions were detected between 425 and 475 nm (405/425-475), while SyBr Green I was excited with a 494 nm laser and emission was detected at 519 nm (494/519). Observations were performed in two siliques and two pistils.

2.12. Quantification of funiculus length

Pistils previous emasculated and siliques were collected, the valves were removed and the remain biological material was cleared in 1 M NaOH and stained with 1% Calcofluor White M2R, as described before. The samples were placed on a microscope slide and mounted in water, so that the funiculus could be as straight as possible. Maximum intensity projections taken with LSM780NLO confocal microscope (Zeiss) and processed with ZEN software (Zeiss) were analysed with Image J software (Schneider *et al.*, 2012). Representative pictures were from 18 WT and 15 *stk* funiculi (among two plants) from stage 12 flowers and 17 WT and 19 *stk* funiculi (among five plants) from stage 17 flowers. Straight lines were designed along the funiculus to measure its length. The statistical significance of the differences was assessed using a Student's t-test ($\alpha = 0.05$).

2.13. Imaging Processing

Regarding scale bars and small image adjustments, all images were processed using the software Image J (Schneider et al., 2012).

3. Results

3.1. Bioinformatics analysis

With the aim of identify putative CRPs targets of STK, the transcriptomic data of *stk* inflorescences (Mizzotti *et al.*, 2014) was crossed with available lists of CRPs under-predicted in plants (Silverstein *et al*., 2007) and CRPs found in *A. thaliana* WT ovules (Huang *et al*., 2015).

stk RNA sequencing (RNA-seq) data contained 17741 genes from which only 1822 genes had a significant *p*-value ($p < 0.05$). These DEGs were crossed with CRPs lists and the results showed that 3.8% of the genes present in the *stk* transcriptome are CRPs. Only 10 genes were common to the three sets of data, 57 genes were found in the *stk* and CRPs from ovules data, 3 genes were exclusively in the *stk* inflorescences and in the list of predicted CRPs in plants, and 134 genes were expressed in both CRPs lists (Figure 7).

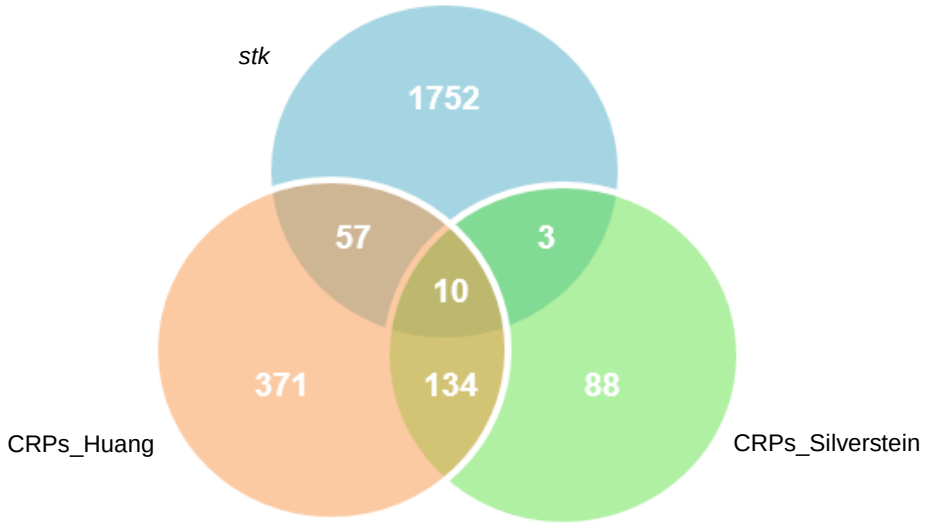

Figure 7. Venn diagram representing the crossing of Differentially Expressed Genes of *stk* RNA sequencing (*stk*) with CRPs under-predicted in plants (CRPs_Silverstein) and CRPs found in *A. thaliana* WT ovules (CRPs_Huang).

From the lists obtained by overlapping *stk* transcriptome with CRPs data, the genes that were presented in the 3 sets of data and the ones only present in *stk* and in one of the CRPs lists were selected. After filtering the genes by choosing a False Discovery Rate (FDR) below 0.05, each gene was briefly described, using TAIR (http://www.arabidopsis.org/). Additionally, the putative expression pattern of the genes

was also investigated based on the e-FP Browser tool (http://bar.utoronto.ca/efp/cgi-bin/efpWeb.cgi), Klepikova Arabidopsis Atlas e-FP Browser (Klepikova *et al.*, 2016) and on Huang *et al.* (2015), which grouped the CRPs into six different clades: CRPs enriched in immature ovules (A), in mature ovules (B), in pollinated ovules (C), in fertilized ovules at two successive stages (D and E) and during early seed development (F). This step was performed in order to find genes preferentially expressed in reproductive tissues. With the information collected, some interesting genes were selected to further be subject of study.

Overall, the *stk* transcriptome presented genes, which belong to different CRPs classes: DEFL, RALF, LTP, ECA1, etc. Among the CRP genes existing in *stk* inflorescences and with a FDR < 0.05 (Table 4), the gene with the highest fold change (6.1x) was *AT1G56415*. This gene has not yet been described and so, the only information available was the expression pattern according to Huang *et al.* (2015), which included this gene in pattern D clade (mainly expression on fertilized ovules). *LCR73* and *AT1G13605* were the next two genes with the highest fold change (4.9x). Their expression was mainly on seeds. *AT2G43530* and *RALFL24* were two genes that, even though with a lower fold change in *stk* data (3x and 2.1x, respectively), their expression pattern was quite interesting since it was similar to STK's (highly expressed in ovary tissues). In this list, most of the genes were mainly expressed in reproductive tissues, after fertilization stages. It is worth noting the fact of some CRPs from Table 4 have a sequence similarity to the pollen coat protein gene family (LCR73, LCR38, LCR48, LCR68) or to the male component of the self-incompatibility response (SCRL10) gene family.

Table 4. List of genes encoding for CRPs present in *stk* RNA sequencing (*stk*-WT). Gene locus, Log_2 of fold change (FC), a brief description of the gene's function, the gene expression pattern according to Huang *et al.* (2015) and the expression profile according to eFP Browser and Klepikova Arabidopsis Atlas eFP Browser are detailed for each gene. Huang *et al.* (2015) defined six distinct expression patterns: CRPs enriched in immature ovules (A), in mature ovules (B), in pollinated ovules (C), in fertilized ovules at two successive stages (D and E) and during early seed development (F). It is also presented the false discovery rate (FDR) for *stk* RNA-seq (FDR < 0.05). The list is organized in a descendant order according to the fold changes in the *stk* RNA-seq.

	stk-WT					
Gene	Log_2FC	FDR	Gene description	Expression Pattern	Gene expression	Reference
AT1G56415	2.6	0.00	Expressed protein	D		
AT2G02147	2.3	0.00	*LCR73, LOW-MOLECULAR-WEIGHT CYSTEINE-RICH 73.* Protein with sequence similarity to the pollen coat protein gene family	D	Higher expression in seeds from silique 5	Vanoosthuyse *et al.* (2001)
AT1G13605	2.3	0.00	Defensin-like (DEFL) family protein	D	Highly expressed in seeds from silique 5 and 7	
AT4G15735	2.2	0.00	*SCRL10, SCR-like 10.* Protein with sequence similarity to S locus cysteine-rich protein	D	Higher expression in seeds from silique 7	Vanoosthuyse *et al.* (2001)
AT4G19905	2.2	0.00	*LCR38, LOW-MOLECULAR-WEIGHT CYSTEINE-RICH 38.* Protein with sequence similarity to the pollen coat protein gene family	D	Higher expression in seeds from silique 7	Vanoosthuyse *et al.* (2001)
AT1G58055	2	0.00	DEFL family protein	D	Higher expression in seeds from the silique 7	
AT3G48231	1.9	0.00	*LCR48, LOW-MOLECULAR-WEIGHT CYSTEINE-RICH 48.* Protein with sequence similarity to the pollen coat protein gene family	F	Highly expressed in seeds	

Gene	*stk*-WT Log_2FC	FDR	Gene description	Expression Pattern	Gene expression	Reference
AT1G58055	2	0.00	DEFL family protein	D	Higher expression in seeds from the silique 7	
AT5G01870	1.9	0.00	Lipid transfer protein (PR-14) family	D	Highly expressed in seed and root without apex	Tung *et al.* (2005)
AT3G01323	1.8	0.01	ECA1-like. Gametogenesis related family protein	F	Expression mainly in seeds	
AT2G22055	1.7	0.04	*RALFL15*, *RALF-LIKE 15*	A		Campbell *et al.* (2017)
AT2G43530	1.6	0.00	Scorpion toxin-like knottin superfamily protein	C	Higher expression in the ovary tissues and seed coat	
AT3G08770	1.4	0.01	*LTP6*, *LIPID TRANSFER PROTEIN 6.* Lipid transfer protein (PR-14) family	F	Expression mainly in seeds	Tsai *et al.* (2016)
AT2G02130	1.2	0.01	*LCR68/PDF2.3*, *LOW-MOLECULAR-WEIGHT CYSTEINE-RICH 68.* Plant defensin family	D	Highly expressed in root, shoot apical meristem and in the flower stage 9	Vanoosthuyse *et al.* (2001)
AT3G23805	1.1	0.01	*RALFL24*, *RALF-LIKE 24*	E	Higher expression in the 2nd internode of the stem, stigma, ovaries and seed coat	Campbell *et al.* (2017)

At the same time, a manual analysis on *stk* transcriptome was performed. The purpose was not only to look for CRPs that did not appear when the transcriptomes were crossed, but also receptors with a kinase domain and other genes deregulated in *stk* inflorescences and possibly thrilling to study in the future. Once again, a description of each gene along with the expression pattern was performed when possible. Analysing Table 5, the gene with the highest absolute fold change (4.3x) was *AT5G63087*, a CRP that was not identified on the previous analysis and whose expression is specific on seeds. *SERINE CARBOXYPEPTIDASE- LIKE 41* (*SCPL41*) was downregulated 1.5x in the absence of STK, with a correspondent FDR < 0.05. Although *SCPL41* is not a CRP or receptor, it is a gene to take in account as a possible player of STK network, since both share a very similar expression pattern. From this list, the genes with a FDR above 0.05 were *NET3C*, *RALFL8*, *RALFL9* and *LCR69*. Again, a link between STK and the male reproductive tissues was found, since CRPs specifically expressed on pollen grain and PT were upregulated on the *stk* transcriptome.

One of the objectives of the present work was to obtain a transcriptome from ovule's sporophytic tissues, where STK is localized. Therefore, the bioinformatics analysis performed was a starting point on understanding if STK could possibly be regulating genes related to peptide signalling such as CRPs. The information collected will be very helpful for the analysis of specific transcriptomic data from integuments and/or funiculus cells.

Table 5. List of genes deregulated in *stk* RNA sequencing (*stk*-WT). Gene locus, Log_2 of fold change (FC), a brief description of the gene's function, and the expression profile according to eFP Browser and Klepikova Arabidopsis Atlas eFP Browser are detailed for each gene. It is also presented the false discovery rate (FDR) for *stk* RNA-seq. The list is organized in an ascendant order according to the fold changes in the *stk* RNA-seq.

	stk-WT				
Gene	Log_2FC	FDR	Gene description	Gene expression	Reference
AT5G42230	-1.5	0.00	*SCPL41*, *SERINE CARBOXYPEPTIDASE-LIKE 41*. Serine carboxypeptidase-like family	Highly expressed on ovary tissue	Fraser *et al.* (2005)
AT2G47920	-0.7	0.27	*NET3C*, *NETWORKED 3C*. Kinase interacting (KIP1-like) family protein	Specifically expressed on seeds from silique 5 and 7	Wang *et al.* (2014)
AT2G02100	0.8	0.20	*LCR69*, *LOW-MOLECULAR-WEIGHT CYSTEINE-RICH 69*. Plant defensin family	Mainly expressed on seeds (endosperm) and shoot apex	Vanoosthuys *et al.* (2001)
AT1G61563	0.7	0.1	*RALFL8*, *RALF-LIKE 8*	Specifically expressed on pollen grains and pollen tube	Campbell *et al.* (2017)
AT1G61566	1.8	0.03	*RALFL9*, *RALF-LIKE 9*	Specifically expressed on pollen grains and pollen tube	Wang *et al.* (2008)
AT5G63087	2.1	0.00	Plant thionin family protein	Specifically expressed on seeds from silique 5 and 7	

3.2. Methods for the isolation of different ovular cells/nuclei

To isolate integuments and/or funiculus cells/nuclei from *A. thaliana* ovules, different experiments were performed, which will be explained below. Depending on the situation, flowers from two distinct development stages, 12 and 17 (according to Smyth *et al.*, 1990), were used. Stage 12 is characterized by a rapidly lengthen of petals, followed by a growth of stamens and gynoecium. The anthers almost reach maturity and ovules are mature, prepared to be fertilized. The sepals open, allowing seeing a small portion of the petals. Stage 17 begins when the floral parts fall from the green silique, which already harbours seeds. The stage ends when the silique turns yellow.

3.2.1. Isolation of protoplasts from ovule's sporophytic tissues

To obtain a transcriptome from a specific tissue it is necessary to separate cells/nuclei from the desire tissue. One way of doing that is by obtaining protoplasts from the wanted tissue. Then, if a cell type-specific fluorescent reporter line for that tissue is used, FACS (Fluorescence activated cell sorting) can separate the marked cells from the solution.

Therefore, the first approach chosen was the protoplasts isolation from integuments and funiculus tissues. Three distinct enzymatic solutions were tested in WT ovules from flowers at stage 12 with different exposition times, in order to find out which combination suited the best to our purpose (Figure 8). The WT ovules were exposed to solution 1 for 1 and 2 hours (Figure 8 A and A', respectively). In both cases, when analysed under the microscope, it could be seen some cell detachment in the funiculus tissue. However, the integuments practically looked the same, not showing any signs of enzymatic activity. For solution 2 (Figure 8 B), two known enhancers of enzymatic activity, BSA and $CaCl_2$, were added to disrupt integuments cell walls. After 1 hour incubation with this new solution, it was possible to see a considerable amount of funiculus cells being released, when compared to the previous case. Regarding integuments, it was still not evident the detachment of the cells. Sporadically, some cells near the integuments' limits appeared to be being released, but not in enough number. Moreover, some big, round cells, resembling the central cell from the megagametophyte were also found in the solution. In the final tested solution, solution 3 (Figure 8 C and C'), the concentration of maceroenzyme and pectolyase was increased as well as the incubation time. The ovules were exposed to the solution overnight. The results showed that protoplasts from

funiculus were perfectly released. Remarkably, protoplasts from integuments could not be found. A closer look into the images helped to see that integument cells shape was becoming rounder, looking like they were going to detach. Yet, the cell wall from integuments remained intact. Once again, central cells were found near the ovules.

Unfortunately, the experiment of isolating protoplasts from ovule's sporophytic tissues was not successful and so, neither the *pSTK:STK-GFP* marker line nor the FACS technique was utilized.

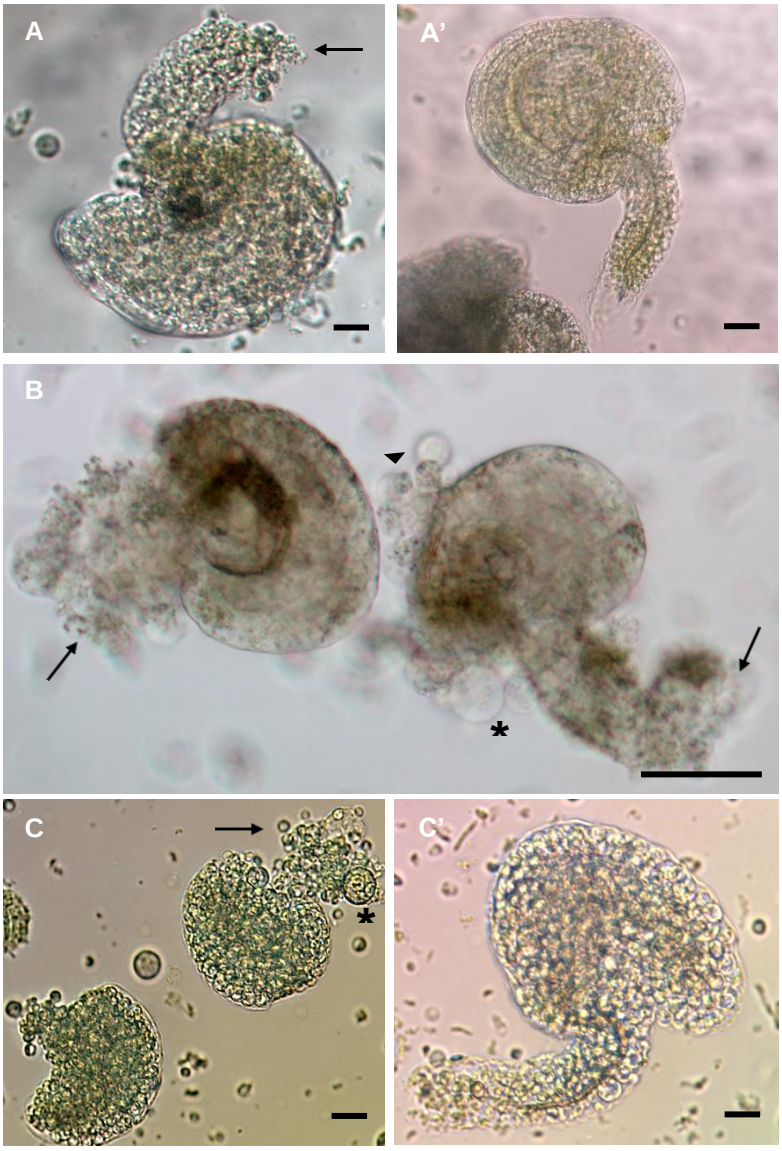

Figure 8. Isolation of protoplasts from WT ovules of *A. thaliana*. Ovules from stage 12 flowers (according to Smyth *et al.*, 1990) were released into distinct enzymatic solutions with different incubation times. **(A, A')** WT ovules put on solution 1 for 1 and 2 hours, respectively. **(B)** WT ovules incubated on solution 2 for 1 hour. **(C, C')** WT ovules after overnight incubation on solution 3. The black arrows indicate protoplasts from funiculus. The black arrowhead illustrates integument cells being released. The asterisk (*) represents the central cell from megagametophyte. Scale bars = 50 µm.

3.2.2. Nuclei isolation from ovule's sporophytic tissues

Since the plant's cell walls can be very resistant to cell wall digestion, the isolation of nuclei from a specific tissue can be a way of obtaining a cell type-specific transcriptome profile. Briefly, by extracting nuclei from a cell specific reporter line with fluorescence, it is possible to separate the labelled nuclei using FANS (Fluorescence activated nuclei sorting).

The experiment started by isolating nuclei from WT leaves, using the NPB solution, and confirm under the microscope if, indeed, nuclei were being isolated. Before checking, DAPI was added to the sample, which is a known fluorescent stain for DNA. It was possible to see many small, blue dots, which did not have the shape and size of a leaf's nuclei (Figure 9 A and A').

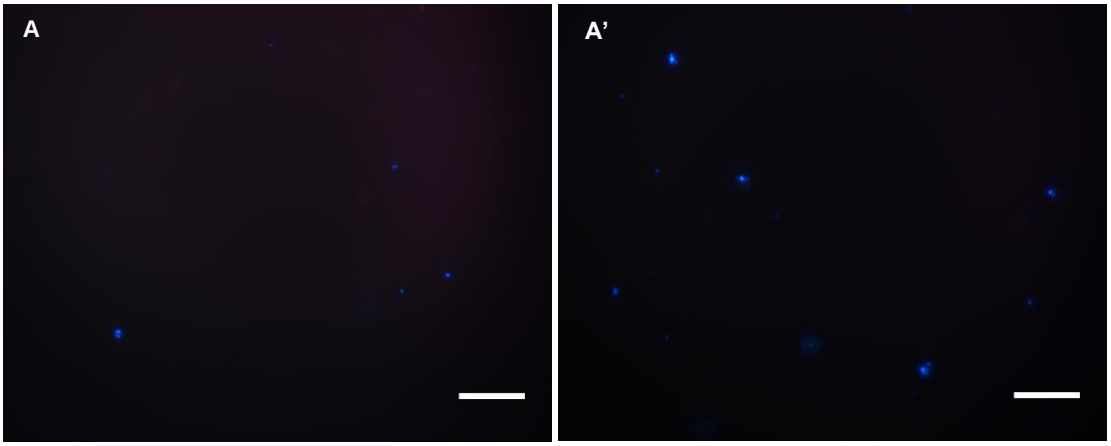

Figure 9. Nuclei isolation inspection from *A. thaliana* WT leaves. (A, A') After isolation of nuclei using WT leaves as starting material, the solution was stained with DAPI. Nuclei were checked under a fluorescent microscope using DAPI channel. It was observed many blue dots whose size was smaller than the expected for nuclei as well as the shape: not the typical round shape. Scale bars = 50 µm.

Even though this result was not as expected, *Arabidopsis* leaves nuclei sorting was performed using FANS. Nuclei from leaves of an available marker line in the laboratory, *ATML1::NLS-VENUS*, were isolated following the same procedure as for WT leaves. Once again, DAPI was added to the nuclei solution. The solution was then sorted by DAPI and GFP channel. However, no nuclei could be found, when checking the quality of the filtered solution.

Once *pSTK:STK-GFP* plants reached floral development stage 12, it was possible to use ovules from this line to try to isolate nuclei and see if the GFP signal appeared. Firstly,

the GFP signal was checked under the fluorescent microscope. As can be seen, the GFP protein could be detected in all the ovules (Figure 10 A). A closer look showed STK-GFP signal present in the ovule's sporophytic tissues, integuments and funiculus (Figure 10 B). Although the signal was not too strong, it was enough to be detected and so, the ovules were used for the nuclei extraction. A new nuclei isolation buffer (NIB) was used, and samples were stained with DAPI. In the samples, it was possible to observed two different structures. In Figure 10 C and C', small round dots were detected. The DAPI and the GFP signal did not look specific. On the other hand, as it can be seen in Figure 10 D and D', bigger dots were found. GFP and DAPI signal detected from these dots looked very diffuse. Lastly, before adding the NIB, the ovules marked with GFP were fixed in order to prevent the disruption of the nuclear membrane. However, the results ended up being the same as the ones already reported (Supplemental Figure 1). It was possible to see many dots from where the signal of DAPI and GFP appeared and spread. The nuclei isolation strategy did not work for isolating nuclei from funiculus and integuments.

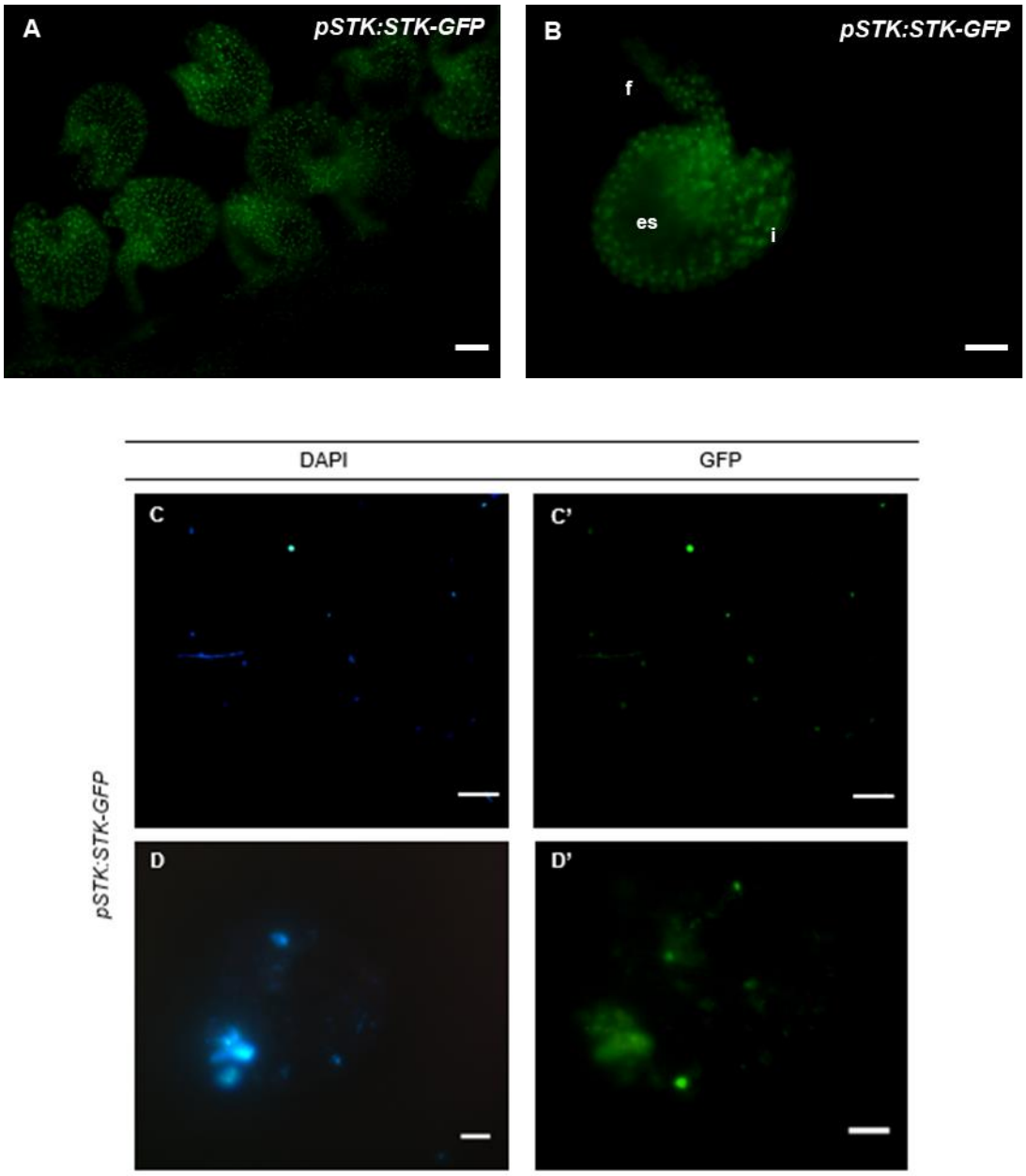

Figure 10. Examination of nuclei isolation quality from *pSTK:STK-GFP A. thaliana* ovules. *pSTK:STK-GFP* ovules from stage 12 flowers (according to Smyth *et al.*, 1990) were used. GFP signal was detected in all the analysed ovules **(A)**, being specific to the ovule's integuments and funiculus **(A')**. Nuclei isolation was checked under the fluorescent microscope using DAPI **(C, D)** and GFP channel **(C', D')**. One observation consisted in small round dots with a non-specific signal. In the other case, it was seen some bigger dots with the DAPI and GFP signal being widely dispersed. es - embryo sac; f - funiculus; i - integuments. Scale bars = 20 µm for (B); 30 µm for (C, C', D, D'); 50 µm for (A).

3.2.3. Obtaining a funiculus transcriptome

3.2.3.1. New procedure to isolate living funiculus cells

Since *STK* is one of the few genes known to be expressed in the funiculus, affecting the development of this tissue, it was decided that a comparison between WT and *stk* transcriptome from this tissue would be an interesting approach. To analyse the possibility of STK involvement in the production of signal molecules for PT guidance, funiculi from stage 12 flowers were collected. It is already known that STK not only affects funiculus size in ovules from flowers stage 17, but also participates in the formation of a correct SAZ in the funiculus, at the same stage, likewise *stk* funiculi from stage 17 were also isolated.

When observing ovules from stage 12 and 17 under the stereomicroscope, it was evident that the funiculus' size was enough to allow manually handle and, most important, it was possible to separate the funiculus from the other ovule's tissues. According to these features, a novel procedure for living funiculus cells isolation was designed (Figure 11). Under a stereo microscope, pistils at stage 12 were first dissected and ovules were placed into a 50 µL droplet of medium in a plastic dish (Φ 3.5 cm). With a surgical knife, each funiculus was separated from the ovule and, then, transfer with a tungsten needle to another plastic dish containing 10 µL of medium. This step was important to avoid contamination of the funiculus samples. Finally, each funiculus was transfer to an eppendorf tube, which already had 40 µL of RNAlater™ Stabilization Solution (Ambion).

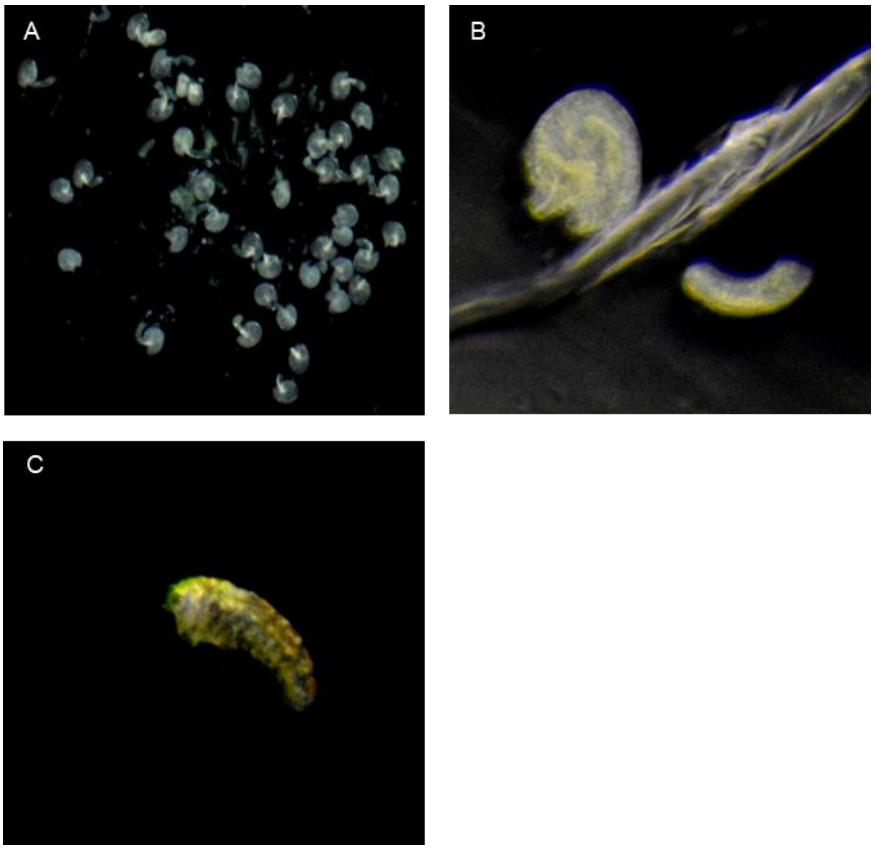

Figure 11. Procedure for funiculus cells isolation, using stage 12 flowers (according to Smyth *et al.*, 1990). Succinctly, under a stereo microscope, ovules were placed in a plastic disk containing 50 µL of medium **(A)**. Each funiculus was cut using a surgical knife **(B)** and each one was transferred to a new plastic disk containing 10 µL of medium **(C)**. This last step helped in avoiding contamination of the funiculus sample by cells of other ovule's tissues.

3.2.3.2. Assessment of funiculus cell mRNA quality

At this point, it was unknown how many funiculi should be collected and used for mRNA extraction, in order to achieve enough amount of mRNA and proceed to cDNA library preparation. Hence, several samples with different number of funiculi were obtained from WT flowers at stage 12 as well as samples containing total ovules from 5 pistils. From those samples, mRNA was extracted using the Dynabeads™ mRNA DIRECT™ Micro Kit (Invitrogen) and its quality was measure by an Alignment 2100 Bioanalyzer. Samples 1, 2, 4, 5, and 7 represent mRNA extracted from 10, 40, 35, 20 and 50 funiculi, respectively. Sample 9 denotes ovules from 5 pistils. Samples 3, 6, 8 and 10 are replicates of samples 2, 5, 7 and 9, respectively. Table 6 indicates the RNA concentration of each sample. In general, the mRNA concentration was very low, compared to the

qualitative range of the equipment (250-5000 pg/µL). Sample 9, containing total ovule, presented the highest mRNA concentration value (69 pg/µL), while sample 3 (with 40 funiculi) and 7 (with 50 funiculi) had the lowest one (3 pg/µL). Among the samples containing only funiculi, sample 8, with 50 funiculi, showed the highest value, 49 pg/µL. It is worth noticing in the discrepancy of mRNA concentration between a sample and its replicate. From this analysis we could at least see that there was no problem with mRNA extraction, since no contamination from ribosomal RNA (rRNA) was found in the samples (Supplemental Figure 2).

Table 6. Assessment of funiculi cells mRNA quality. mRNA concentration (pg/µL) was obtained using an Alignment 2100 Bioanalyzer. Samples 1, 2, 4, 5, and 7 represent mRNA extracted from 10, 40, 35, 20 and 50 funiculi, respectively. Sample 9 contains ovules from 5 pistils. Samples 3, 6, 8 and 10 are replicates of samples 2, 5, 7 and 9, respectively. Overall, the mRNA concentration was very low (< 250 pg/µL). Sample 9 had the highest value and sample 3 and 7 had the lowest. Sample 8 was the one with the highest value among the samples containing only funiculi. All the biological material used are from flowers at stage 12 (according to Smyth *et al.*, 1990).

	Sample									
	1	2	3	4	5	6	7	8	9	10
mRNA Concentration (pg/µL)	33	42	3	22	10	28	3	49	69	29

Another attempt for funiculi isolation was performed. This time, 100 funiculi from WT ovules at each stage, 12 and 17, were isolated, following the procedure described before. Again, mRNA from the two samples were extracted and it was immediately used as template for cDNA synthesis, using the High-Capacity RNA-to-cDNA™ Kit (ThermoFisher).

To address the problem of funiculus cDNA quality and possible contamination by other cells, a semiquantitative RT-PCR was performed. *ARABINOGALACTAN PROTEIN 9* (*AGP9*) had been reported as present in the funiculus, although with some expression in the chalaza pole of the ovule (Pereira *et al.*, 2014). On the other hand, *SUCROSE SYNTHASE 4* (*SUS4*) was reported as being specifically expressed in funiculus cells, after fertilization (Khan *et al.*, 2015). To test possible contamination by tissues near the funiculus, it was used *AGP4*, whose expression was found in the integuments (Pereira *et al.*, 2016), and *FERTILIZATION INDEPENDENT SEED 2* (*FIS2*), a specific protein for

central cell and endosperm (Luo *et al.*, 2000). The *ACTIN 7* (*ACT7*) was used as a positive control (housekeeping gene). Whenever it was possible, the primers were designed to distinguish cDNA from gDNA amplified.

Concerning to stage 12, Figure 12 demonstrates that *AGP9* primers correctly amplified funiculus cDNA. The same occurred when *ACT7* primers were used. Apparently, no contamination from integuments and central cell happened, since *AGP4* and *FIS2* primers could not amplify cDNA from funiculus, but they were able to do so when ovules cDNA and gDNA were used. *SUS4* primers did not amplify funiculus cDNA. Ovules cDNA might be contaminated with gDNA because a product with the expected gDNA size appeared when *FIS2* and *SUS4* primers were used with cDNA as template.

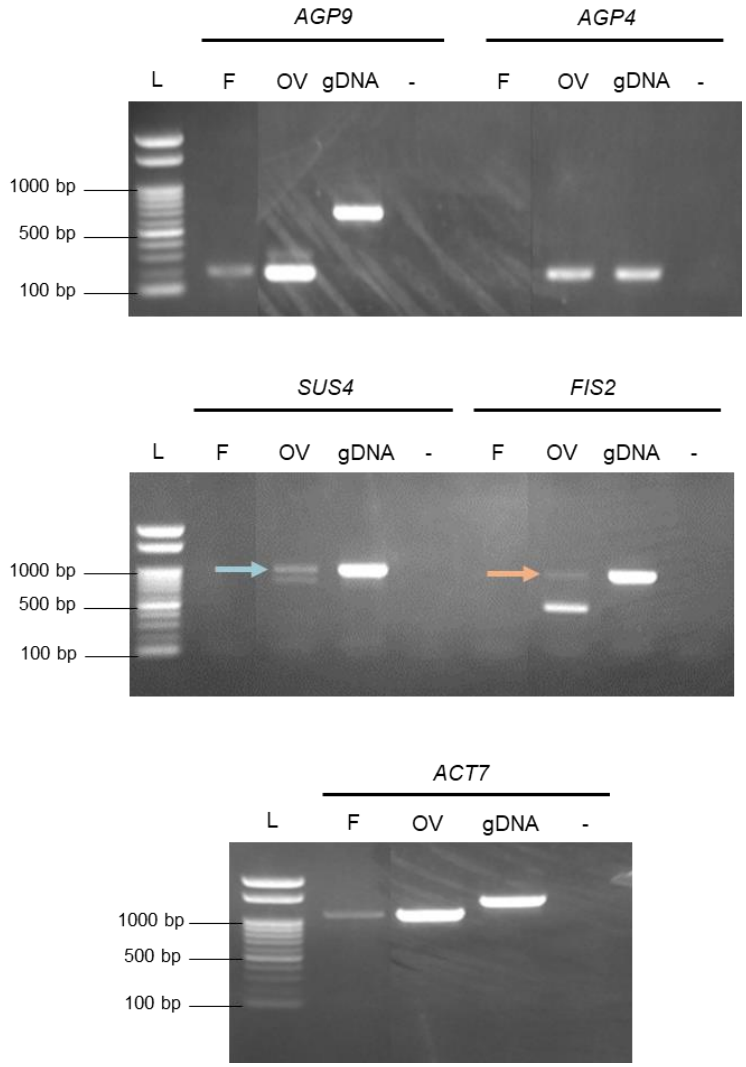

Figure 12. Electrophoretic analysis of semiquantitative RT-PCR from funiculus of WT flowers at stage 12 (according to Smyth *et al.*, 1990). *AGP9* is expressed on funiculus and chalaza pole of the ovules; *AGP4* is specific of ovule's integuments; *SUS4* is specific for funiculus after fertilization; *FIS2* is expressed in the central cell and endosperm; *ACT7* was used as a positive control. An expected band size for gDNA when using *SUS4* (blue arrow) and *FIS2* (orange arrow) primers appeared in the ovule's cDNA sample. F - cDNA from funiculi; OV - cDNA from ovules; gDNA - genomic DNA; L – Molecular DNA weight ladder; – negative control without DNA.

Regarding stage 17 (Figure 13), once again funiculus cDNA was amplified by *AGP9* primers with the expected size (197 bp) and by *ACT7* primers with the expected size of 1109 bp. *AGP4* primers did not amplified any product from funiculus cDNA and the same happened with *FIS2* primers as well as with *SUS4* primers. These primers amplified products when ovules cDNA and gDNA were used.

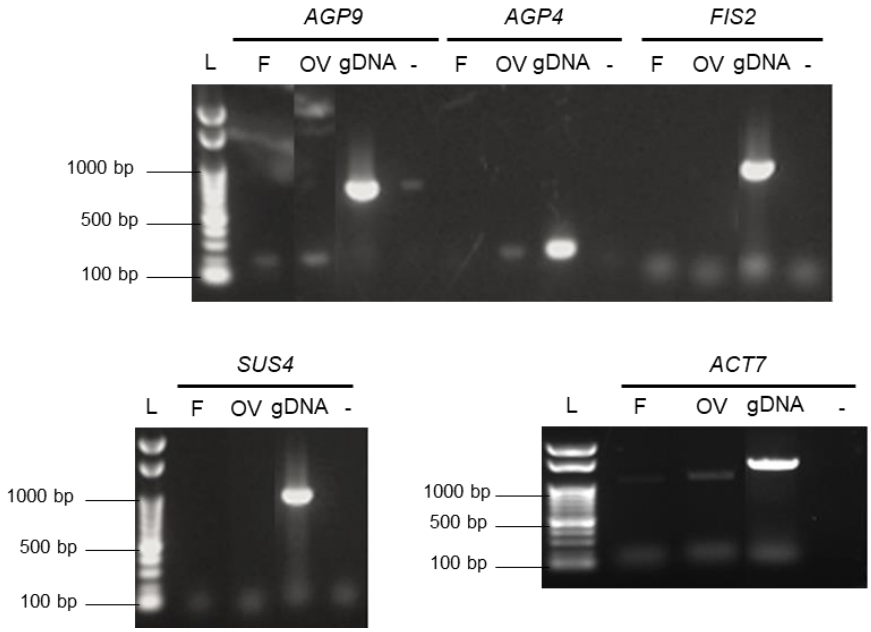

Figure 13. Electrophoretic analysis of semiquantitative RT-PCR from funiculus of WT flowers at stage 17 (according to Smyth *et al.*, 1990). *AGP9* is expressed on funiculus and chalaza pole of the ovules; *AGP4* is specific of ovule's integuments; *SUS4* is specific of funiculus after fertilization; *FIS2* is expressed in the central cell and endosperm; *ACT7* was used as a positive control. F - cDNA from funiculi; OV - cDNA from ovules; gDNA - genomic DNA; L – Molecular DNA weight ladder; – negative control without DNA.

3.2.3.3. RNA-sequencing library preparation

Taking in account the results from the RT-PCR, it was decided to proceed for RNA-seq library preparation in order to test if an enough number of reads would be obtained from the sequencing.

The experiment designed was as described in Figure 14: WT and *stk* funiculi from flowers at stages 12 and 17 were collected; each of the four samples contained 100 funiculi, extracted following the procedure described in Figure 11; mRNA was extracted from each sample, and the library preparation was performed using TruSeq® RNA Sample

Preparation Kit V2 (Illumina Inc.). The four samples were sent for sequencing. PCR analysis confirmed *stk* plants as having a mutant allele (Supplemental Figure 3).

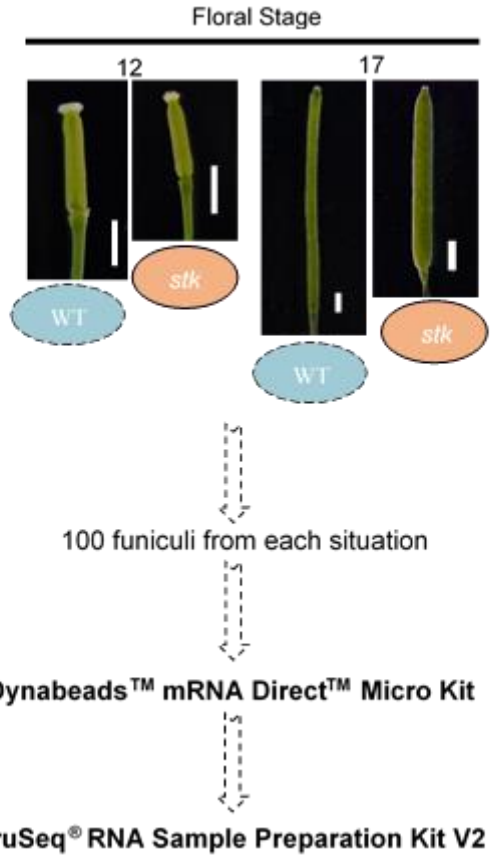

Figure 14. Experimental design for RNA-seq of funiculi samples. Briefly, 100 funiculi were collected from WT and *stk* flowers at stages 12 and 17 (according to Smyth *et al.*, 1990), each. Dynabeads were used for mRNA extraction and TruSeq RNA Sample Preparation Kit V2 was used for RNA-seq library preparation. Scale bars = 1 mm.

The sequencing results demonstrated that stage 12 *stk* sample had 372620 reads and WT sample had 99950 reads, while stage 17 *stk* sample had 13435972 reads and the WT one 11693548 reads. Therefore, only the samples containing funiculi from fruits at stage 17 had enough number of reads, and consequently, they could be mapped against *Arabidopsis* cDNA, showing a 90% (*stk* sample) and 87% (WT sample) correspondence. The experiment proceeded focusing on stage 17. Two biological replicates from *stk* and WT funiculi samples were collected as well as three samples with ovules from 5 *stk* and WT pistils. All the samples were sent for sequencing and the results obtain are being analysed for future studies.

3.3. Phenotypic analysis of *stk* mutant during ovule development

It was important to quantify *stk* phenotype regarding PT guidance as well as funiculus development during floral stages 12 and 17 (according to Smyth *et al.*, 1990), from which funiculi were previously isolated for transcriptome analysis. Those are two main stages where funiculus function is probably essential. This has not been reported and would facilitate the analysis of the funiculus transcriptomes, relating phenotype with the genes deregulated in the *stk* mutant compared to the WT.

3.3.1. Analysis of STK involvement in PT guidance - aniline blue staining

STK is a TF present on the funiculus cells from the moment this stalk structure arises until seed dehiscence occurs. Evidences points that some molecules involved in PT-pistil interactions might be produced on the funiculus cells. To address the question if STK might be regulating the expression of such molecules in the funiculus, WT PTs growth and guidance in *stk* mutants were observed using DAB staining. DAB is a callose-specific fluorochrome, which labels the PTs cell walls as well as the callose plugs that PTs periodically produced along their growth, to keep the cytoplasm near the PT tip.

In this experiment, observations of WT PT growth along WT and *stk* pistils, previously emasculated, were performed. In both situations (Figure 15 A and C), the pollen grains had an efficient germination on the surface of the stigma and the PTs grew correctly along the pistil until they reached the embryo sac. In the WT, as expected, only one PT entered in each ovule (Figure 15 D). The results from crossing WT pollen with *stk* flower (Figure 15 B) showed an identical phenotype: only one PT entering in each ovule.

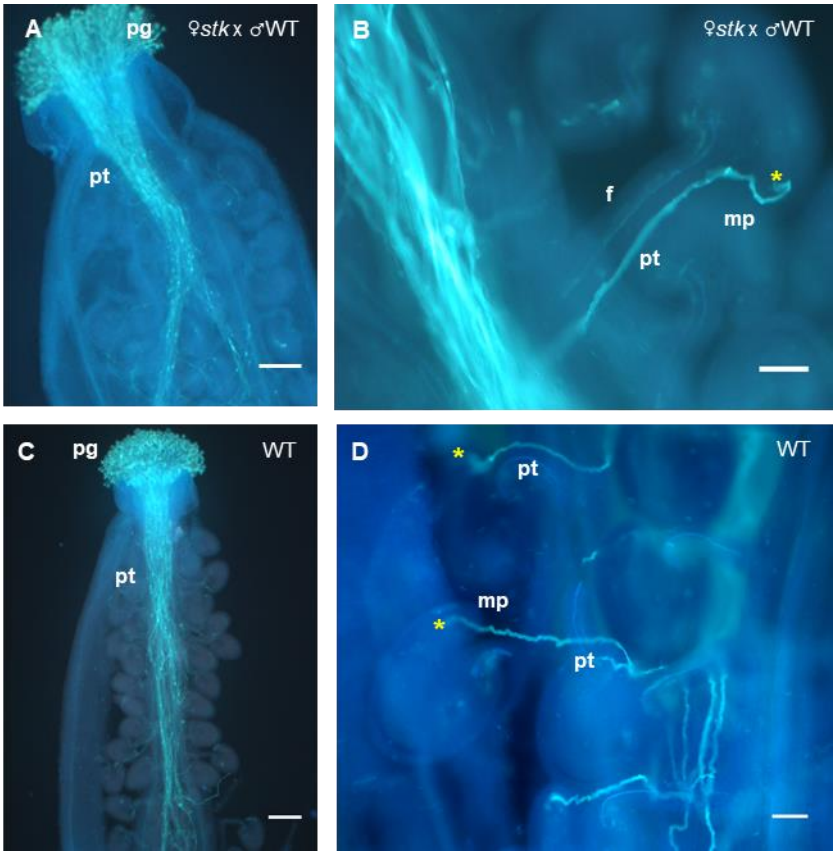

Figure 15. Aniline blue staining of WT pollen tubes. **(A, C)** Pollen grains germinated correctly on the stigma surface of a *stk* and WT pistil, respectively. Pollen tubes grew normally through the style tissues. **(B)** Cross between a female *stk* flower and wild type pollen, where a single pollen tube entered in the ovule (yellow asterisk). **(D)** A single pollen tube entered the embryo sac of a wild type ovule (yellow asterisk). f - funiculus; mp - micropyle; pg - pollen grain; pt - pollen tube. Scale bars = 50 µm.

3.3.2. Analysis of STK involvement on funiculus growth

It is known that a wild type funiculus goes through an increase in its size after double fertilization, at floral stage 17. In *stk,* the increase in funiculus size is qualitatively greater than in WT, at stage 17. Nevertheless, there is no quantification of *stk* funiculus size compared to the WT. Importantly, it is unknown whether this effect occurs prior to fertilization, namely at stage 12. To answer these questions, two approaches were considered: measuring the funiculus length and calculate the number of cells that composed this sporophytic tissue.

3.3.2.1. Finding the ideal method for funiculus stained

For both funiculus growth quantification strategies, it was required staining the cell walls from all funiculus cells because it would allow a high-resolution imaging throughout the entire structure. Due to that, three distinct dies were tested. SR2200, a dye for imaging of whole ovules, was used for ovules from stage 12 flowers. However, the stained was not able to penetrate in the tissues (Figure 16 A') and only the cells on the surface of the funiculus were correctly outlined (Figure 16 A). PI staining revealed that only the cells located in the periphery of the tissue were outlined (Figure 16 B). Once again, the stain could not penetrate deep into the tissue. For last, ovules were cleared and stained with 1% Calcofluor White M2R. In this case, it was also tested which type of microscopy would be more appropriate: confocal or two-photon. Calcofluor White M2R was capable to stain all cells, but the image taken with two-photon microscope (Figure 17 A') was not so cleared compared to the confocal one (Figure 17 A): the limitation of funiculi cells shape on the first case was not entirely visible as happened in the confocal image.

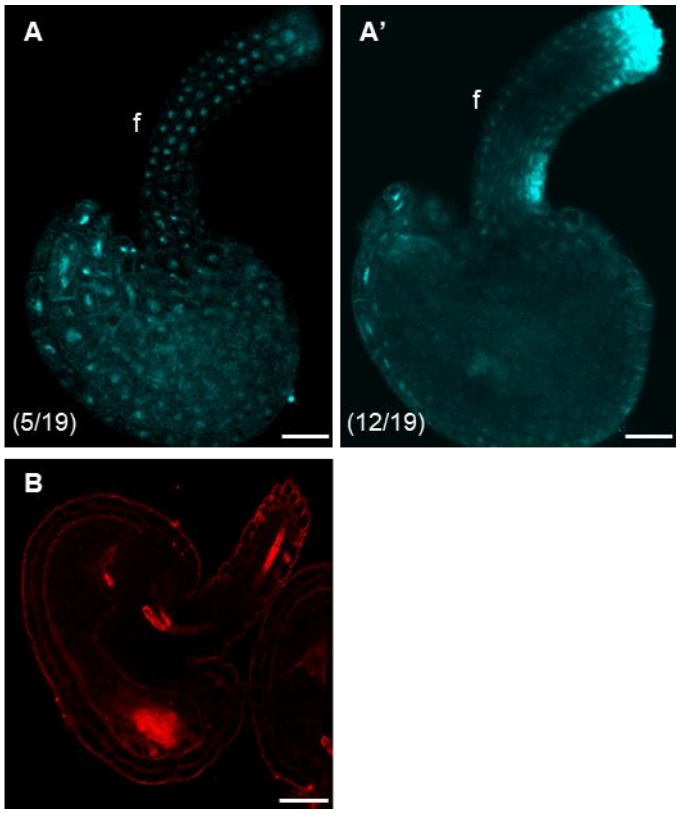

Figure 16. Confocal laser-scanning images of WT ovules stained. Staining the funiculus cell walls with SR2200 was only effective on cells located on the surface of the tissue **(A)**. The dye could not penetrate into deeper cells of funiculus **(A')**. The numbers in parenthesis represent the z-sections. **(B)** PI staining of funiculus cell walls just stained the cells present in the periphery of the tissue. Image is an optical section, taken with a confocal microscope. Ovules used are from flowers at stage 12 (according to Smyth *et al.*, 1990). f - funiculus. Scale bars = 20 µm.

In order to count the cell number of a funiculus, nuclei had to be stained. Pistils at stage 12 were cleared and stained with Calcofluor White M2R and SyBr Green I (Figure 17 B). The limits of the funiculus cell walls were visible using the Calcofluor White M2R staining. However, the SyBr Green I signal looked scattered, not being possible to see the usual round shape of nuclei. Unfortunately, due to time restrictions, it was not possible to continue this experiment and try another type of nuclei staining to count the cell number.

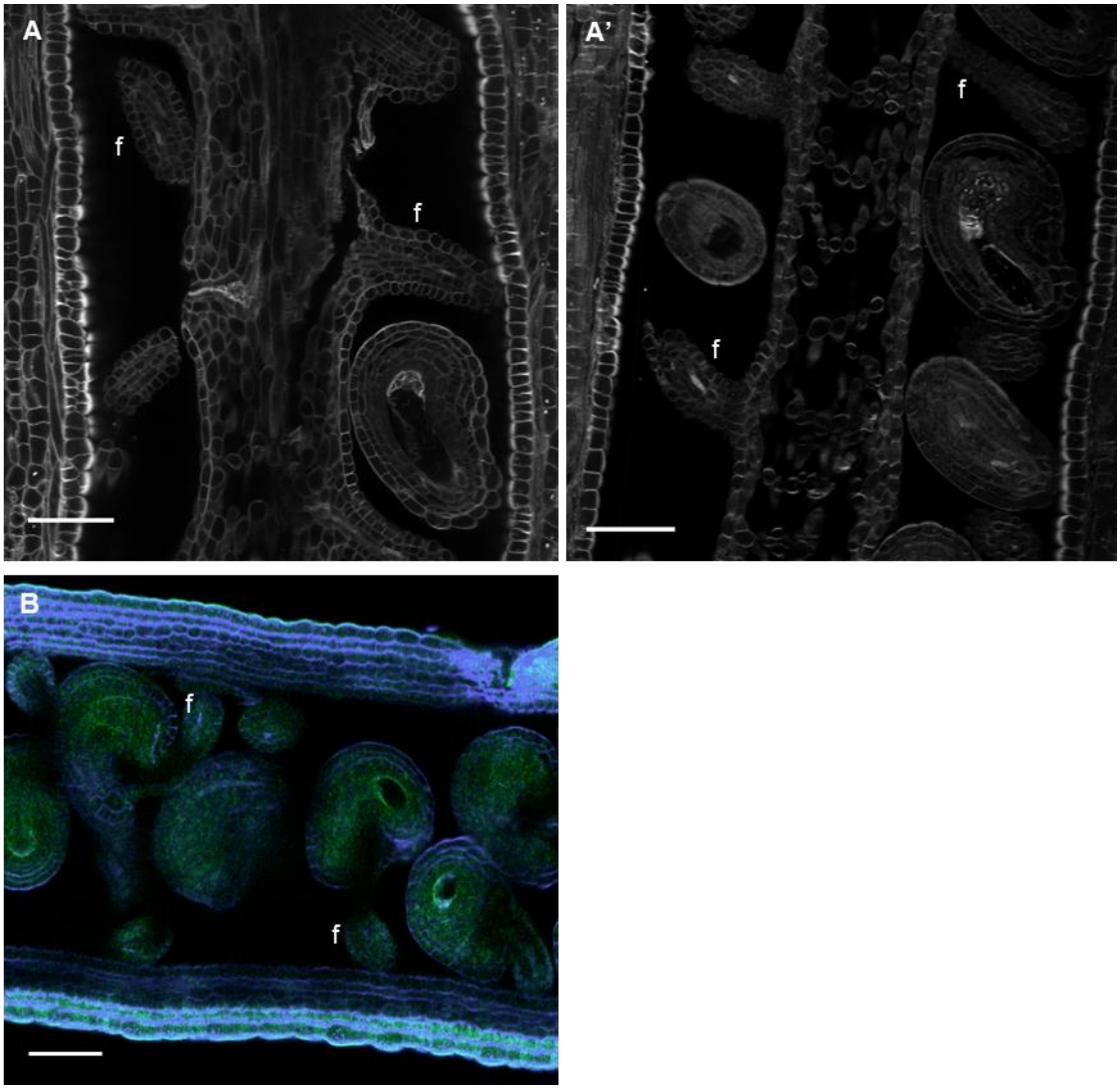

Figure 17. Images of stained WT pistils. Comparison between confocal **(A)** and two-photon **(A')** imaging of pistils stained with Calcofluor White M2R. Confocal imaging showed a better resolution of funiculus cells compared to two-photon. **(B)** Confocal imaging of a pistil, whose cell walls were stained with Calcofluor White M2R (purple) and nuclei were stained with SyBr Green I (green). SyBr Green I staining did not looked specific to the nuclei since it did not show the usual round shape of a nucleus. WT pistils were from stage 12 flowers (according to Smyth *et al.*, 1990). f - funiculus. Scale bars = 50 µm.

3.3.2.2. Quantification of funiculus length

To measure the funiculus length, the strategy adopted consisted on clearing and staining ovules with Calcofluor White M2R, take maximum projection images of them, using a confocal microscope, and measure the funiculus length with an image-processing program, as shown in Figure 18.

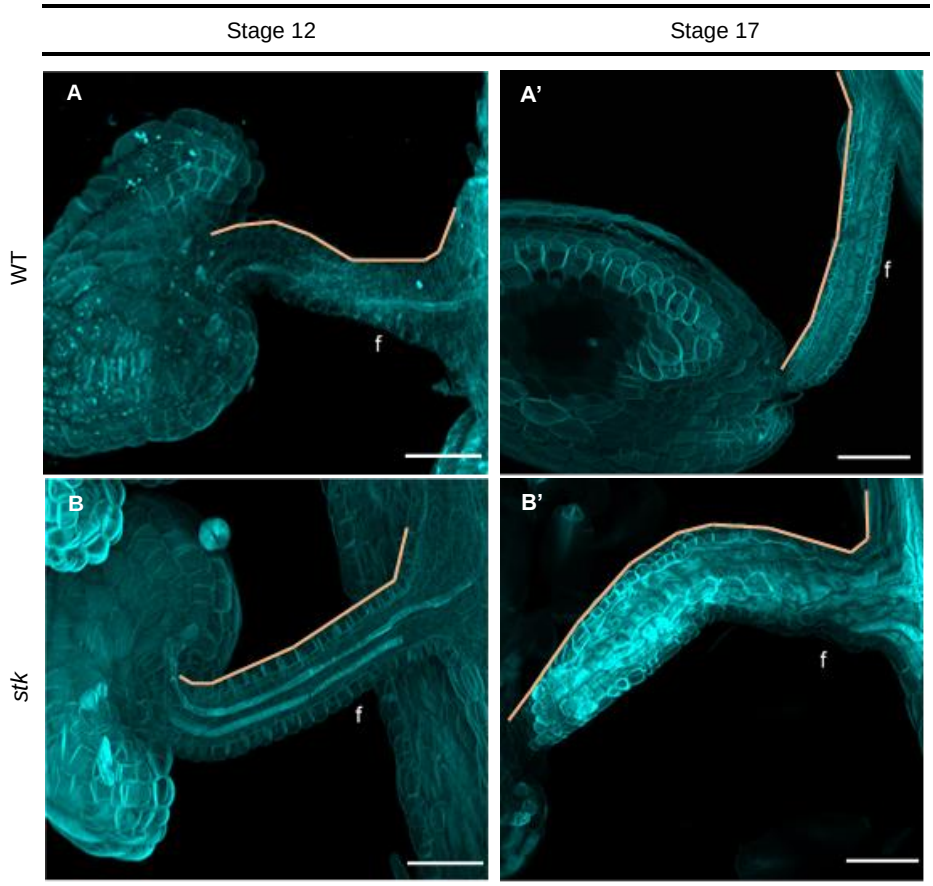

Figure 18. Maximum-intensity projections of confocal z-stacks of *A. thaliana* ovules. Using Image J, straight lines (orange line) were drawn along the funiculus to measure its length. **(A)** WT funiculus from stage 12. **(A')** WT funiculus from stage 17. **(B)** *stk* funiculus from stage 12. **(B')** *stk* funiculus from stage 17. Stages 12 and 17 are according to Smyth *et al.* (1990). f - funiculus. Scale bars = 50 µm.

Figure 19 demonstrates the results obtained from the analysis of 18 WT and 15 *stk* funiculi (among two plants) from stage 12 flowers and, 17 WT and 19 *stk* funiculi (among five plants) from stage 17 flowers. The results indicated that the length of a WT funiculus is 128.46 µm, whilst the length in the *stk* mutant funiculus is 152.23 µm. No statistically significance differences appeared between the length on WT and *stk* funiculi from stage 12 plants. When a transition from ovule to seed occurred, the funiculi show an increased in length: both WT and *stk* have 2 times increase. However, at stage 17, the mutant's funiculi (with a length around 320 µm) showed an increase in size compared to the WT funiculi (around 235 µm).

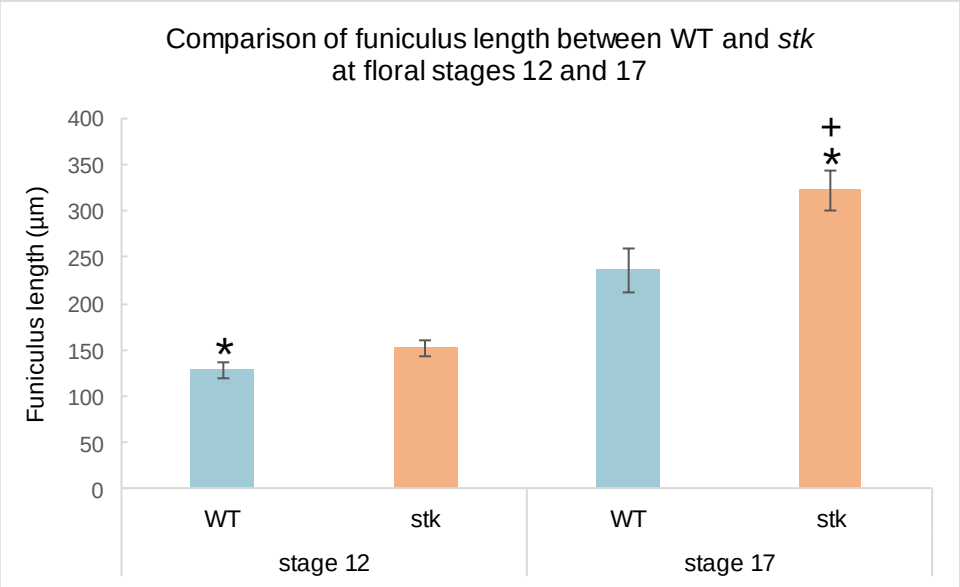

Figure 19. Comparison of funiculus length between WT and *stk*, from flowers at stages 12 and 17 (according to Smyth *et al.*, 1990). Error bars are the (±) standard error. A Student's t-test was performed, α = 0.05. * indicates statistical differences when compared to WT at stage 17. + indicates statistical differences when compared to *stk* at stage 12.

4. Discussion

The present work was focused on understanding the involvement of peptide signalling in processes controlled by STK. A bioinformatics analysis on *stk* transcriptome was performed, to understand if a link between STK and peptide signalling existed. Some interesting genes were found and further studied in a detail *in silico* analysis (4.1. Bioinformatics analysis). Since no peptide-receptor pairs acting in the ovule's sporophytic tissues were reported yet, the second aim was to obtain a transcriptome from integuments and funiculus, from floral stage 12 and 17 (4.2. Methods for integuments and funiculus cells/nuclei isolation). Afterwards, the data would be analysed to discover genes regulated by STK and related to peptide signalling. Finally, the participation of STK in processes happening in the tissues selected for the transcriptome as well as involving the stages selected was investigated. PT guidance was analysed by aniline blue (4.3.1. Analysis of STK involvement in PT guidance) and the funiculus size was quantified (4.3.2. Analysis of STK involvement on funiculus growth). This multistep study will contribute to unveil STK network.

4.1. Bioinformatics analysis

As reviewed in the introduction, evidence points out for a cross talk between the sporophyte and megagametophyte since the start of ovule development, until the formation of a seed. Peptide signalling is a plausible way of communication because ligands are small molecules capable of moving from cell-to-cell. However, no ligand-receptor pair has been reported in ovule's sporophytic tissues. STK is a transcription factor that controls processes of ovule and seed development, being highly expressed on the female sporophytic tissues, integuments and funiculus (Mizzotti *et al.*, 2014). For this reason, *stk* RNA-seq DEG list was overlapped with two available lists of genes from *A. thaliana*, which encode for CRPs (a class of peptides which encompasses most of the peptides identified in pollen-pistil interactions). The intention was to understand if STK could be affecting the expression of CRPs and therefore, confirm the possible involvement of STK with peptide signalling.

The cross of transcriptomes revealed that only 3.8% of the genes in the *stk* DEG list encodes for CRPs. This percentage includes genes present in both CRPs lists used (CRPs_Huang and CRPs_Silverstein) or in just one of them. For the analysis of the list

obtained, only the genes with a FDR < 0.05 were taken in account. Statistically, genes with an FDR below 0.05 means that the differences found in the gene expression, in this case between *stk* mutant and WT, are significant. The analysis of Table 4 revealed many CRPs classes (LCR, DEFL, RALF), whose genes have not yet been described. On one hand, it means that most of them could be potential genes to study in the future. However, the lack of *in silico* information does not help in understanding what the protein function could be or in which type of processes it could be involved. For example, *AT1G56415* was the gene with the highest fold change in *stk* transcriptome (6.1x) with a significant FDR (FDR = 0.00). It certainly could be a putative gene regulated by STK. Nevertheless, the only information found for this gene was the expression pattern according to Huang *et al.* (2015), which classified the correspondent CRP as being enriched in fertilized ovules. The class of CRPs that *AT1G56415* belongs to is still unknown, which complicates further studies about gene function. Online tools were used to understand if the listed genes were related to reproduction and to *STK* expression pattern. By consulting the expression pattern on eFP Browser and Klepikova Arabidopsis Atlas eFP Browser, it was found that most of the genes were mainly expressed on seeds, where STK is expressed. Interestingly, it looks like two genes were preferentially expressed before double fertilization: *AT2G43530* enriched in unfertilized ovules, but whose pistil was already pollinated, and *RALFL15* enriched in immature ovules. Concerning the first gene, it belongs to the scorpion toxin-like knottin superfamily protein, encoding for an ion channel inhibitor. It is known that ion oscillations occur during PT-pistil interactions and even inside the ovules, namely in the synergid cells, egg cell and central cell (Hamamura *et al.*, 2014). Perhaps, STK might be controlling the ion oscillations that occur inside the ovules at the time of PT arrival. On the other hand, RALFs are peptides already reported as players in plant's reproduction. If *RALFL15* expression happens mainly in immature ovules, this gene may be important for the success of ovule development. Continuing in the RALFs family, although *RALFL24* fold change was low (2.1x), its expression pattern on eFP Browser revealed to be very similar to the *STK* one (a high expression on ovary tissues). This made us wonder about a possible direct interaction between *STK* and *RALFL24*. Even though STK has always been associated with female-related processes, curiously, CRPs with a protein sequence similar to pollen coat protein family and to S locus cysteine-rich protein family were found among *stk* transcriptome data. This leads to speculate if STK may regulate

genes that not only function on female development, but also on male reproductive development.

A manual analysis on *stk* RNA-seq was also performed in an attempt to find other genes that were not present in the CRPs lists used before. The criteria to select interesting genes was genes with a *p*-value below 0.05 and with expression on reproductive tissues. From all the genes listed in Table 5, the most interesting one was *SCPL41*, which belong to a serine carboxypeptidase-like clade II family (Fraser *et al.*, 2005). This gene is downregulated in the *stk* mutant and its expression pattern in plant tissues is very similar to the *STK* one, being expressed mainly in the pistil tissue and in early seed development stages. Furthermore, a study in which a specific serine carboxypeptidase, *Extra Carpels and Seeds 1*, was overexpressed showed an increased number of seeds and carpels per silique (Wen *et al.*, 2012). This demonstrates that the serine carboxypeptidase-like family might be implicated in reproductive processes. Once again, a link between STK and the male reproductive tissues was established. *RALFL8* and its paralog, *RALFL9*, are two genes highly expressed in the mature pollen grain, continuing along the pollen germination phase and the consequently PT. The transcriptomic values for *RALFL8* were not reliable since its FDR is above 0.05. However, *RALFL9* was 3.5- fold upregulated in *stk* transcriptome with a FDR = 0.03. Therefore, STK regulation of genes related to male reproduction should be an interesting subject of investigation.

This bioinformatics analysis demonstrated that a relationship between STK and peptide signalling exists, since several CRPs are deregulated in the *stk* transcriptome. The genes found will be investigated in the transcriptome from ovules' sporophytic tissues to see if they are expressed there.

4.2. Methods for integuments and funiculus cells/nuclei isolation

4.2.1. Protoplasts isolation from ovule's sporophytic tissues

One of the techniques developed to allow the study of the transcriptome from a specific cell type was the generation of protoplasts from GFP-expressing plants, following FACS, to separate the mixed population of cells based on fluorescent properties. Even though this technique has been used for more than 40 decades, the problem is that isolation of protoplasts in *A. thaliana* are mostly from leaf mesophyll (Abel *et al.*, 1994; Yoo *et al.*,

2007; Rottmann *et al.*, 2018) or young seedlings cells (Zhai *et al.*, 2009), not being appropriate to other type of cells with different morphology or properties.

Since it has not been reported any protoplast isolation from either ovule's integuments or funiculus cells, the first enzyme solution tried was based on one used to isolate gametophytic cells from *Torenia* (Kawano *et al.*, 2011). The WT ovules were exposed to this solution and after 1 and 2 hours, they were checked under the microscope to see if there were any differences regarding cell detachment. Both cases exhibited the same result: cells were starting to release from the funiculus, but the integuments looked intact, not showing signs of enzymatic activity. Maybe ovules should be exposed to the solution for more than two hours. However, it is also evident that integuments and funiculus do not share an identical morphology with the gametophytic cells from *Torenia* and the fact that this plant species presents a protruding embryo sac facilitates the exposition of the gametophytic cells to the enzymatic solution, allowing protoplasts isolation. Despite knowing the importance of these features for the enzymatic treatment, it was decided to try once again solution 1, but with the addition of $CaCl_2$ and BSA, which are two compounds known for stabilize enzymes in a reaction and consequently, improve their efficiency. This solution was named solution 2 and WT ovules were exposed to it for 1 hour. The results showed a much considerable number of funiculus cells dethatching, compared to the ovules in solution 1. Occasionally, it was possible to see the effects of enzymes in the integuments cells walls, but the isolation of protoplasts was not evident. The fact that the micropyle region was affected by the enzymes' activity led to the release of a big round cell that was the central cell. It is clear that adding $CaCl_2$ and BSA to the solution helped in improving the enzymes activity, at least concerning the funiculus cells. The integuments are sporophytic tissues composed of several compacted cell layers, since one of the functions of integuments is to protect the megagametophyte. Interestingly, ovule integuments and leaves display similarities in a morphological, molecular and structural level, such as organ initiation, bilateral symmetry and determinant of growth (Pillitteri *et al.*, 2007; Kelley and Gasser, 2009). Therefore, the next enzymatic solution tested, solution 3, was based on a previous one applied to isolate leaf mesophyll protoplasts (Yoo *et al.*, 2007), but with some modifications made by Park *et al.* (2016). This time, the ovules were incubated overnight and checked under the microscope. The analysis of the pictures allowed concluding that funiculus cells detached and it would be possible to isolate them. Concerning to integuments, it was not observed

any protoplasts from these tissues. Some of the ovules exhibit the integuments cells with a rounder shape than the usual, but the cell wall remained intact. Once again, central cell isolation was observed, which was in fact the purpose of Park *et al.* (2016), when they used this solution. Even though the overnight exposure did not function, maybe it should not be used for this type of study, because it may cause stress to the ovule's cells, inducing a stress responsive gene expression, which will alter the normal transcriptome. Perhaps, increasing the enzymes concentration could help in disrupting integuments cell walls. Adding a vacuum step during incubation with the enzymatic solution could also resolve the problem, since the infiltration of the solution through the tissues could be better.

4.2.2. Nuclei isolation from ovule's sporophytic tissues

To overcome the problem of cell walls resistant to enzymatic digestion, the strategy used was the nuclei isolation. This technique has a homogenization physical process that allows disrupting the cells from any tissue. Then, nuclei labelled with a fluorescent protein from the broken cells can be recover and purify from the solution by FANS.

There is some reticence about using nuclear RNA as a source of transcriptional information from the whole cell. Studies comparing total RNA pool with nuclear RNA showed that only a small fraction of genes (around 3%) was significantly accumulated at different levels between the nucleus and the cell (Barthelson *et al.*, 2007; Zhang *et al.*, 2008). Thus, the transcript abundancy in nuclei and cell are correlated (Jacob *et al.*, 2007; Deal and Henikoff, 2010). That is why it is plausive to consider this technique in order to obtain a transcriptome from ovule's sporophytic tissues.

The isolation of nuclei from leaves were the first to be tested since protocols optimized were available for using this type of tissue as biological material (Deal and Henikoff, 2011). The analysis of the results allowed concluding that nuclei were not being isolated. Using WT leaves together with NPB, it was found under the microscope some structures stained with DAPI, but they did not resemble nuclei. They were small dots with a much smaller size compared to leaf's nuclei, which usually have a 10 µm diameter. Furthermore, the experiment of nuclei isolation from *ATML::NLS-VENUS* leaves, followed by cell sorting with FANS, did not show any nuclei, when analysed under the

microscope. A problem during the nuclei sorting could have happened but there is also the possibility that the method itself was not being performed correctly.

pSTK:STK-GFP ovules from stage 12 plants (according to Smyth *et al.* 1990) exhibited the GFP signal in both integuments and funiculus cells. The observations made under the microscope showed, once again, small dots, like the ones previously referred, in which the signal from DAPI and the GFP did not look specific. This time, some bigger dots were found, whose emitted signal looked very diffuse. DAPI binds to DNA and the GFP protein is reporting the presence of STK that as a TF is present in the cell's nucleus. For this reason, it was expected to visualize an overlapping of DAPI and GFP signal, which did not occur. The NIB used in this experiment contained Triton X-100, a reagent that enhances the release of nuclei from cells and prevents the nuclei from clumping (Loureiro *et al.*, 2007). However, if the concentration of the detergent in the solution is too high as well as the exposition time of the samples to it, the nuclear membrane will be disrupted (Carrier *et al.*, 2011). Since it was not found any protocol for nuclei isolation from ovules or more specifically from integuments and funiculi, one possible explanation for the results observed can be the fact that Triton X-100 concentration used or the time the material was exposed to it was not the ideal one for this case. A pre-fixation of the ovules with a paraformaldehyde solution was also done with the aim of avoid nuclear membrane disruption. However, the results observed were similar to the ones without the fixation. It was found many dots that revealed a DAPI and GFP signal, which was spreading away.

Nuclei isolation from integuments and funiculus tissues was not possible to obtain. The hypothesis that technical issues may reflect these unusual results for nuclei cannot be discarded. The solution would be proceeding with the optimization of the process, which requires time to perform more experiments.

4.2.3. Transcriptome from funiculus: procedure and mRNA quality evaluation

The new procedure for funiculus cells extraction was based on the principle that the funiculus could be manually separated from the rest of the ovule, under a stereomicroscope. In this technique, the ovules were placed in a medium (Gooh *et al.*,

2015), which was previously used for live-cell imaging of *Arabidopsis* embryogenesis, because it was the one with the highest percentage of ovule survival. Moreover, the droplet of this medium stayed intact during the procedure, which helped in extracting each funiculus with the tungsten needle. After being cut, each funiculus was transferred to another small droplet of medium. By placing the funiculus in the new droplet, it was possible to verify if contamination from other type of cells was occurring. If so, the funiculus would be cleaned in the new droplet and then transferred to the eppendorf tube containing RNAlater. This tissue storage reagent was used to stabilize and protect the cellular RNA, while the others funiculi were being extracted. Since this procedure is a little time-consuming, it was important to find a solution, which would minimize the need to immediately process the sample or to freeze it in liquid nitrogen. This procedure filled the requirements of tissue-specific extraction without jeopardizing the quality of the RNA.

The mRNA quality from the several samples, containing different amounts of funiculi was not satisfactory. All of them showed a very low mRNA concentration that did not reach the lowest range of the equipment that is 250 pg/µL. The sample containing only ovules was the one with the highest concentration. This result was expected since the ovule is a structure composed of more cells than a funiculus and consequently, it will contain more mRNA. Among the funiculi samples, the highest concentration of mRNA was extracted from 50 funiculi. Therefore, more than 50 funiculi should be collected for extraction of enough mRNA. We cannot ignore the possibility of a problem with the manual maceration of the funiculi during mRNA extraction, because sometimes the funiculi would stay attached to the walls of the tube and thus, the pestle was not able to macerate it. From the measurement of mRNA quality, contamination from rRNA was not found, which reflected the proper use of the dynabeads kit used for mRNA extraction. The bioanalyzer software uses data from total RNA to determine the RNA Integrity Number (Schroeder *et al.*, 2006). In our experiment, only samples containing mRNA were analysed with the bioanalyzer. That is why this parameter of RNA integrity evaluation was not considered.

Analysis of a semiquantitative RT-PCR using primers specific for a given tissue is also a strategy adopted to verify not only the quality of mRNA extraction but also if contamination of the samples occurred. In both situations, in which 100 funiculi from both stage 12 or 17 plants (Smyth *et al.*, 1990) were collected, a low intensity band with the expected size was amplified when primers specifically for *AGP9* were used [Pereira *et*

al. (2014) reported *AGP9* as expressed in the funiculus and chalaza pole of the ovule]. The same was seen with primers for *ACT7*. This leads to speculate if these two genes have a normally low expression in the funiculus or if the amount of cDNA synthesized from this tissue was too low. No contamination from integuments or central cell was found in funiculus samples since *AGP4* and *FIS2*, respectively, were not amplified from funiculus cDNA. On the contrary, ovules cDNA and gDNA were amplified, showing that the lack of a band when funiculus cDNA was used as template cannot be justify due to problems with the primers or the reaction. This result demonstrates the efficiency of the new procedure in avoiding contamination from other ovule's tissues by transferring each funiculus to a new droplet before placing it inside the eppendorf tube. *SUS4* is a gene identified as specifically expressed in the funiculus cells by analysis of transcriptomic data from this sporophytic tissue (Khan *et al.*, 2015). The relative abundance of *SUS4* decreases from globular to mature green stage of seed development. That is why it was not expected to find an amplified when funiculi from stage 12 plants were used. However, an amplified should had appeared when stage 17 funiculi cDNA was used. Since the sample containing total ovules cDNA was also not amplified, but the one with gDNA was, a problem with the technique during cDNA addition to the PCR tubes seemed to be a reasonable explanation.

4.2.3.1. RNA-sequencing library: from preparation to preliminary results

The presence of STK during funiculus development is quite intriguing because it leads to questioning the importance of this TF's function in the funiculus. Indeed, Pinyopich *et al.* (2003) revealed that STK participates in cell division and expansion processes in the funiculus and Balanzà *et al.* (2016) results were a starting point on disclosing how STK is controlling the proper formation of the SAZ. However, all the players involved in these processes have not yet been described. Therefore, a comparison between WT and *stk* transcriptome concerning floral stage 17 is of interest. On the other hand, evidences (revised in the introduction) demonstrated that some peptides or small molecules existing in the funiculus might be important for the PT orientation journey. Since *STK* is expressed in the funiculus during that time, there is a possibility that it can be regulating the expression of such molecules. No transcriptome from WT funiculi before fertilization

occur exists so, obtaining a transcriptome from WT and *stk* funiculi at floral stage 12 would clarify which type of genes are involved in the STK network and which ones are normally expressed in the WT funiculus.

Only the samples containing funiculi from stage 17 plants had enough reads and could be mapped against the *Arabidopsis* cDNA. Several factors might had influenced these results. First, the morphology of a funiculus from stage 12 plants is different from funiculus at stage 17. They are smaller in length and cell number, which, in turn, makes it more difficult to macerate and extract enough mRNA for cDNA library preparation. The RNA-seq library preparation kit used might had not been the best choice for samples with low amount of mRNA. The input quantity recommended for the TruSeq® RNA Sample Preparation V2 kit (Illumina Inc.) is between 10-400 ng of mRNA. However, the samples that were sent for sequencing were not quantified in the bioanalyzer due to cost-effective issues. Therefore, it is possible that the mRNA extracted from funiculi at floral stage 12 did not reach the minimum threshold required for this kit and so the experiment did not work well. The possibility of technical effects cannot be discarded, as well, because the library preparation requires several ligations of adaptors and PCR amplifications, which by themselves are techniques with a risk of failure associated (Fang and Cui, 2011). Perhaps, in a nearby future, it would be of interest to extract more funiculus from stage 12 plants or performed an amplification step before the library preparation. However, it must be considered that there are several commercially available kits for RNA amplification and so, a decision would have to be made regarding which kit would be better to our purpose. The kit used for the RNA-seq library preparation was the only one available in our laboratory and that is why the experiment proceeded with it.

It was decided to proceed the experiment only with samples from stage 17. Two biological replicates of funiculi from stage 17 fruits of both WT and *stk* mutant and three biological replicates of WT and *stk* ovules from the same stage were sent for sequencing. The results have been received and at the time of the thesis delivery, they are being analyzed. It is expected to identify genes that are part of the STK network, which controls processes in the funiculus such as cell division and expansion and the establishment of a correct SAZ. It will also be analyzed the involvement of STK in other processes in the funiculus that have not been described yet. Peptide signalling related genes will also be considered in the comparative study of the WT and *stk* funiculi transcriptome. Finally, a

comparison of our data with other available transcriptomic data from other ovule's tissues will allow the identification of genes specifically expressed in the funiculus during floral stage 17. Since the transcriptome from funiculi at floral stage 12 was not obtained, it was not possible to further analyzed the STK involvement in PT guidance at a transcriptomic level.

4.3. Phenotypic analysis of *stk* mutant during ovule development

4.3.1. Analysis of STK involvement in PT guidance

To investigate whether pollen tubes were attracted by the mutant ovules, and if they correctly entered the micropyle, aniline blue staining of WT and *stk* mutant pistils was performed. The results showed that PTs reached all the *stk* ovules and entered the micropyle, indicating that this first part of the fertilization process was not affected. This does not mean that the orientation process of the PTs by the mutant pistil was the same as in the WT one. A semi-*in vivo* assay could clarify this question, as it would be possible to visualize how the PTs were being guided towards the mutant ovule and the time taken for them to find the micropyle, compared to the normal situation, in which a WT ovule is used. As a MADS TF, STK acts in cooperation with other TFs, forming tetramers that will recognize DNA-binding sequences, bind to them and regulate the transcription process. As previous mention in the introduction, SHP1 and SHP2 are TFs that participate in a quartet, together with STK, which are responsible for establishing the ovule identity (Favaro *et al.*, 2003). Moreover, *STK* sequence is extensively similar to the *SHP* genes (Ma *et al.*, 1991) and the analysis of mutants demonstrated that these three TFs have a redundant function (Pinyopich *et al.*, 2003). These premises mean that SHP can replace STK in the quartet and it will still function and recognize the same binding sites in the DNA sequence. This prompts to speculate if the fact of no phenotype concerning PT guidance in *stk* mutant ovules was observed might be due to the lack of STK be masked by the presence of other MADS TFs, which have a similar structure and consequently function. *SHP1* and *SHP2* (previously *AGL1* and *AGL5*, respectively) are also expressed in the integuments and funiculus (Savidge *et al.*, 1995; Flanagan *et al.*, 1996) like *STK*. Therefore, it is possible that they are part of the complex responsible for regulating the expression of molecular cues, important for funicular guidance, and in the absence of STK, they are capable of continuing the regulation of the process.

4.3.2. Analysis of STK involvement on funiculus growth

4.3.2.1. Optimizing the method to stain the funiculus

To be able to quantify the funiculus growth in WT and *stk* mutant, by either measuring the funiculus length or counting the number of cells, it was necessary to stain the cell walls of the funiculus tissue. Cell wall staining with SR2200 was not effective in our case. It did not penetrate deeply in the tissue, therefore all the funiculus cell walls were not outlined. Maybe an increase in the vacuum pressure or in the exposition time to the vacuum could help in the infiltration of the solution through the tissue. The protocol used for SR2200 staining (Musielak *et al.*, 2016) was adapted from the previously published study, Musielak *et al.* (2015). In this work, whole ovule stained images also showed a non-uniformly staining of the cell walls. PI staining was also not able to stain all the funiculus cell walls. Perhaps, increasing the PI concentration and the addition of a vacuum step could resolve this situation. The results clarify that the best stain method would be fixing the pistils and/or siliques, clearing them with NaOH, and, afterwards, stained with 1% CalcoFluor White M2R. ClearSee was also effective in clearing the biological material however, this reagent entails for a prolonged incubation time of the samples. Hence, opting for clearing with ClearSee instead of NaOH was not justified. A simple comparison between confocal and two-photon imaging was also performed to understand which microscope should be used to our purpose. The analysis of the images evidenced that with confocal microscopy it was possible to obtain deeper images of the funiculus with better resolution in which the cells shape of the tissue were clearly outlined, compared to the ones taken with the two-photon microscope. These results are quite interesting because commonly, two-photon excitation microscopy allows deeper penetration of the light, taking high-resolution images of thin optical sections. The explanation might be because in the samples analysed, the valves of the pistils and siliques were not removed. Consequently, to reach the funiculus, the light would have to cross through thick tissues, which would affect the resolution of the two-photon microscope. For this reason, preference was given to the confocal microscope to take confocal image stacks in order to measure the funiculus growth.

To count the funiculus cells with a software, the nuclei of the cells needed to be stained. SyBr Green I, a fluorescent dye that binds to DNA, was tested. The signal emitted from SyBr Green I did not look specific to the cells nuclei. Maybe the concentration of the dye was too low. Despite that, the examination of samples stained with SyBr Green I under

confocal microscopy revealed that the fluorescence faded quickly (Suzuki *et al.*, 1997). Therefore, this stained might not be appropriate for counting the cell number of the funiculus because images would have to be taken rapidly, which in turn could affect the quality of the maximum projections. Time restrictions did not allow continuing testing other DNA dyes and subsequently, the idea of counting the number of cells had to be set aside.

4.3.2.2. Measuring the funiculus growth

After establishing the stained method, funiculi at floral stage 12 and 17 (according to Smyth *et al.*, 1990) from both WT and *stk* were measured as exemplified in Figure 18. This experiment faced two issues. The first one was related to the funiculus shape because normally, they are not in a straight position. A funiculus shows a curvature required for all the ovules or seeds fit inside the pistil or silique, respectively. The solution found was preparing samples in which the valves had been removed from the gynoecium or fruit, depending on the flower stage, and the funiculi remain attached to the septum. This facilitated a manual handling of the funiculi when the slides were being prepared and subsequently, it was possible to place them in a straighter position. The other challenge was to stipulate where the beginning and end of a funiculus is. Since this sporophytic tissue emerges from the septum, it was considered that a small portion of the tissue from where the funiculus emerges was also part of the funiculus. From microscope observations, the funiculus is fused with the remain ovule, meaning that the funiculus ends inside of it. To measure that in these circumstances it was not possible. Therefore, the funiculus was measured until the visible connection with the integuments. This type of analysis is not completely objective. Because of that, a single person performed all the analysis in order to standardize the criterion used.

Projections of confocal image stacks were used to quantify the funiculus length and the statistical analysis revealed some very interesting points. At first, the average length for a WT funiculus before fertilization was 128.46 µm, which is not statistically different when compared to a *stk* mutant funiculus that measured 152.23 µm. This is consistent with the Pinyopich *et al.* (2003) results since they did not report any phenotypic differences in the *stk* funiculi compared to the WT one, at floral stage 12. As it was expected, the seed development is accompanied by an increase on funiculus length because the funiculus

epidermis and cortex cells proliferate to allow the proliferation of the vasculature and so, the nutrition of the developing embryo. Both WT and *stk* funiculi showed a significant increase in length at stage 17. Pinyopich *et al.* (2003) observations revealed that stage 17 *stk* plants presented a longer funiculus, compared to the WT. Therefore, our observations were in accordance since the mutant size was significantly bigger than the WT, after fertilization. *stk* funiculus had a length around 320 µm, while WT funiculus measured 235 µm. Khan *et al.* (2015) also examined the length of the funiculus during seed development in *A. thaliana*. The siliques examined in our study had embryos at globular stage, so the length of the funiculus at this stage was reported to be 260 µm, which was close to the value obtained by us. These results support the STK involvement in the funiculus development, although they did not elucidate if the funiculus increased size observed in the mutant is mostly because of an increase in cell division or in cell expansion. A quantitative and comparative study concerning these two processes between *stk* and WT would be of interest. It is worth noticing that the funiculus growth in the *stk* mutant is only affected after fertilization. This leads to hypothesize that STK control of the funiculus growth occurs in a time-specific manner, in this case, after fertilization takes place. On the other hand, the growth control made by STK apparently is antagonistic because in the funiculus, this TF would be repressing cell division or expansion processes, whilst in the integuments of the seed, STK would activate downstream genes that would promote in a positive way, the same processes, since *stk* seeds are smaller than the WT ones. At the same time, it cannot be discarded the hypothesis that *stk* seeds are smaller due to a repression effect done by a smaller silique.

5. Conclusion

The objective of the present work was to comprehend the involvement of peptide signalling in STK-dependent pathways, acting in processes for the correct seed formation, as well as elucidate the phenotype of the *stk* mutant regarding processes not described yet.

The bioinformatics analysis performed on *stk* RNA-seq suggested that a link exists between STK and peptide signalling. Several CRPs were found deregulated in the *stk* mutant and importantly, the *in silico* analysis showed that these genes are mainly expressed in the reproductive tissues.

Peptide-receptor pairs from ovule's sporophytic tissues have not been described until now. Therefore, this work also focused on trying to obtain a transcriptome for these tissues. The protoplasts isolation was ineffective due to the thicker cell wall that constitutes the integuments cells. The nuclei isolation approach was also not the most suitable for this work. Overall, a transcriptome from integuments cells was not obtained and so, the analysis of putative ligand-receptor pairs controlled by STK and present in the integuments was not achieved.

In this study, an efficient method for living funiculus cells isolation was established. The technique allowed for the collection of pure funiculus cells, which were used for transcriptome analysis. Stage 12 funiculi samples from both *stk* and WT did not have the quality required to obtain the respective transcriptome. Hence, more experiments should be performed to continue studying peptide signalling pathways acting on funiculi during PT-pistil interactions. With these results, it was not possible to uncover, at a transcriptional level, the funiculus function in processes such as PT guidance. On the other hand, the analysis of PT guidance by an aniline blue assay revealed that *stk* ovules mimicked the WT ones, meaning that they were capable of guiding the WT PT into the micropyle. This shows that the lack of STK function, by itself, is not able of disrupt the PT guidance. More experiments should be done to fully understand the PT guidance phenotype in *stk* pistils and if other molecules act redundantly with STK during this process.

The quantitative study regarding funiculus length on both WT and *stk* from stages 12 and 17 plants confirmed that when the seed starts to develop, the *stk* funiculus has an

increased size compared to the WT. However, the quantity and size of individual funiculus cells was not recorded. This analysis allowed to fulfil a gap that existed regarding funiculus morphology, since now there is information about the average size of a funiculus before and after fertilization. The results highlighted the time-specific control of STK in funiculus length because the significant differences in size between *stk* and WT did not happen at stage 12, but only at floral stage 17. The transcriptional data concerning stage 17 funiculi samples is being analysed and, genes deregulated in the mutant and related to cell division and/or expansion are expected to be found. Another important process happening in the funiculi and controlled by STK, at this development stage, is the correct deposition of lignin to establish the SAZ. Thus, our data will contribute to identify genes related to this important process too. Lastly, peptide-receptor pairs acting on the funiculus can also be found, demonstrating that these types of molecules exist in the funiculus.

The funiculus is a fundamental structure, which connects the developing seed with the maternal plant. This tissue possesses numerous plasmodesmata, indicating that cell-to-cell communication occurs frequently. Our transcriptomic data will further contribute to answer some relevant questions: Is peptide signalling involved in funiculus functions? Which other processes is STK controlling in the funiculus? Which genes are specifically expressed in the funiculus? Together, all this information will be important for dissecting the transcriptional machinery of the funiculus, which ultimately contributes for a correct development of the seed and finally, provides essential information for the genomic-level improvement of seed crops.

6. References

Aalen RB, Wildhagen M, Stø IM, Butenko MA (2013) IDA: A peptide ligand regulating cell separation processes in *Arabidopsis*. J Exp Bot **64**: 5253-5261

Abel S, Theologis A (1994) Transient transformation of *Arabidopsis* leaf protoplasts: a versatile experimental system to study gene expression. Plant J **5**: 421–427

Bai L, Ma X, Zhang G, Song S, Zhou Y, Gao L, Miao Y, Song, C-P (2014) A Receptor-Like Kinase Mediates Ammonium Homeostasis and Is Important for the Polar Growth of Root Hairs in *Arabidopsis*. Plant Cell **26**: 1497-1511

Baker SC, Robinson-Beers K, Villanueva JM, Gaiser JC, Gasser CS (1997) Interactions among genes regulating ovule development in *Arabidopsis thaliana.* Genetics **145**: 1109–1124

Balanzà V, Roig-Villanova I, Marzo MD, Masiero S, Colombo L (2016) Seed abscission and fruit dehiscence required for seed dispersal rely on similar genetic networks. Development **143**: 3372-3381

Balasubramanian S, Schneitz K (2000) NOZZLE regulates proximaldistal pattern formation, cell proliferation and early sporogenesis during ovule development in *Arabidopsis thaliana*. Development **127**: 4227–4238

Barthelson RA, Lambert GM, Vanier C, Lynch RM, Galbraith DW (2007) Comparison of the contributions of the nuclear and cytoplasmic compartments to global gene expression in human cells. BMC Genomics **8**: 340

Battaglia R, Brambilla V, Colombo L (2008) Morphological analysis of female gametophyte development in the *bel1 stk shp1 shp2* mutant. Plant Biosyst **142**: 643-649

Becker MG, Hsu S-W, Harada JJ, Belmonte MF (2014) Genomic dissection of the seed. Front Plant Sci **5**: 464

Bedinger PA, Pearce G, Covey PA (2010) RALFs: Peptide regulators of plant growth. Plant Signal Behav **5**: 1342-1346

Belmonte MF, Kirkbride RC, Stone SL, Pelletier JM, Bui AQ, Yeung EC, Hashimoto M, Fei J, Harada CM, Munoz MD, Le BH, Drews GN, Brady SM, Goldberg RB, Harada

JJ (2013) Comprehensive developmental profiles of gene activity in regions and subregions of the *Arabidopsis* seed. Proc Natl Acad Sci USA **110**: 435–444

Bencivenga S, Colombo L, Masiero S (2011) Cross talk between the sporophyte and the megagametophyte during ovule development. Sex Plant Reprod **24**: 113–12

Bleckmann A, Alter S, Dresselhaus T (2014) The beginning of a seed: regulatory mechanisms of double fertilization. Front Plant Sci **5**: 452

Brambilla V, Battaglia R, Colombo M, Masiero M, Bencivenga S, Kater MM, Colombo L (2007) Genetic and Molecular Interactions between BELL1 and MADS Box Factors Support Ovule Development in *Arabidopsis*. Plant Cell **19**: 2544–2556

Brambilla V, Kater MM, Colombo L (2008) Ovule integument identity determination in *Arabidopsis*. Plant Signal Behav **3**: 246-247

Breiden M, Simon R (2016) Q&A: how does peptide signaling direct plant development? BMC Biol **14**: 58

Brown RC, Lemmon BE, Nguyen H, Olsen O-A (1999) Development of endosperm in *Arabidopsis thaliana*. Sex Plant Reprod **12**: 32–42

Campbell L, Turner SR (2017) A Comprehensive Analysis of RALF Proteins in Green Plants Suggests There Are Two Distinct Functional Groups. Front Plant Sci **8**

Carrier G, Santoni S, Rodier-Goud M, Canaguier A, Kochko Ad, Dubreuil-Tranchant C, This P, Boursiquot JM, Le Cunff L (2011) An efficient and rapid protocol for plant nuclear DNA preparation suitable for next generation sequencing methods. Am J Bot **98**: e13–e15

Chan A, Belmonte M (2013) Histological and ultrastructural changes in canola (*Brassica napus*) funicular anatomy during the seed lifecycle. Botany **91**: 671–679

Chen YH, Li HJ, Shi DQ, Yuan L, Liu J, Sreenivasan R, Baskar R, Grossniklaus U, Yang WC (2007) The central cell plays a critical role in pollen tube guidance in *Arabidopsis*. Plant Cell **19**: 3563–3577

Chevalier E, Loubert-Hudon A, Zimmerman EL, Matton DP (2011) Cell-cell communication and signaling pathways within the ovule: from its inception to fertilization. New Phytol **192**: 13–28

Christensen CA, **King EJ**, **Jordan JR**, **Drews GN** (1997) Megagametogenesis in *Arabidopsis* wild type and the *Gf* mutant. Sex Plant Reprod **10**: 49–64

Deal RB, Henikoff S (2010) A simple method for gene expression and chromatin profiling of individual cell types within a tissue. Dev Cell **18**: 1030–1040

Deal RB, Henikoff S (2011) The INTACT method for cell type-specific gene expression and chromatin profiling in *Arabidopsis thaliana*. Nat Protoc **6**: 56-68

Dresselhaus T (2006) Cell-cell communication during double fertilization. Curr Opin Plant Biol **9**: 41–47

Dresselhaus T, Franklin-Tong N (2013) Male-Female Crosstalk during Pollen Germination, Tube Growth and Guidance, and Double Fertilization. Mol Plant **6**: 1018–1036

Drews GN, Lee D, Christensen CA (1998) Genetic analysis of the female gametophyte development and function. Plant Cell **10**: 5–17

DW-K N, Zhang C, Miller M, Shen Z, Briggs SP, Chen ZJ (2012) Proteomic divergence in *Arabidopsis* autopolyploids and allopolyploids and their progenitors. Heredity **108**: 419–430

Edwards K, Johnstone C, Thompson C (1991) A simple and rapid method for the preparation of plant genomic DNA for PCR analysis. Nucleic Acids Res **19**: 1349

Ehlers K, Bhide AS, Tekleyohans DG, Wittkop B, Snowdon RJ, Becker A (2016) The MADS Box Genes *ABS*, *SHP1*, and *SHP2* Are Essential for the Coordination of Cell Divisions in Ovule and Seed Coat Development and for Endosperm Formation in *Arabidopsis thaliana*. PLoS ONE **11**: e0165075

Escobar-Restrepo J, Huck N, Kessler S, Gagliardini V, Gheyselinck J, Yang W, Grossniklaus U (2007) The FERONIA Receptor-like Kinase Mediates Male-Female Interactions During Pollen Tube Reception. Science **317**: 656-660

Ezquer I, Mizzotti C, Nguema-Ona E, Gotté M, Beauzamy L, Viana VE, Dubrulle N, Costa de Oliveira A, Caporali E, Koroney A-S, Boudaoud A, Drouich A, Colombo L (2016) The Developmental Regulator SEEDSTICK Controls Structural and Mechanical Properties of the *Arabidopsis* Seed Coat. Plant Cell **28**: 2478-2492

Fang Z, Cui X (2011) Design and validation issues in RNA-seq experiments. Brief Bioinform **12**: 280-7

FAO (2017) The future of food and agriculture – Trends and challenges. Rome

Favaro R, Pinyopich A, Battaglia R, Kooiker M, Borghi L, Ditta G, Yanofsky MF, Kater MM, Colombo L (2003) MADS-Box Protein Complexes Control Carpel and Ovule Development in *Arabidopsis*. Plant Cell **15**: 2603–2611

Flanagan CA, Hu Y, Ma H (1996) Specific expression of the *AGL1* MADS-box gene suggests regulatory functions in *Arabidopsis* gynoecium and ovule development. Plant J **10**: 343–353

Fraser CM, Rider LW, Chapple C (2005) An Expression and Bioinformatics Analysis of the *Arabidopsis* Serine Carboxypeptidase-Like Gene Family. Plant Physiol **138**: 1136-1148

Ge Z, Bergonci T, Zhao Y, Zou Y, Du S, Liu M, Luo X, Ruan H, García-Valencia LE, Zhong S, Hou S, Huang Q, Lai L, Moura DS, Gu H, Dong J, Wu H, Dresselhaus T, Xiao J, Cheung AY, Qu L (2017) *Arabidopsis* pollen tube integrity and sperm release are regulated by RALF-mediated signaling. Science **358**: 1596-1600

Gooh K, Ueda M, Aruga K, Park J, Arata H, Higashiyama T, Kurihara D (2015) Live-Cell Imaging and Optical Manipulation of *Arabidopsis* Early Embryogenesis. Dev Cell **34**: 242-251

Guan Y, Lu J, Xu J, McClure B, Zhang S (2014) Two Mitogen-Activated Protein Kinases, MPK3 and MPK6, Are Required for Funicular Guidance of Pollen Tubes in *Arabidopsis*. Plant Physiol **165**: 528-533

Hamamura Y, Nishimaki M, Takeuchi H, Geitmann A, Kurihara D, Higashiyama T (2014) Live imaging of calcium spikes during double fertilization in *Arabidopsis*. Nat Commun **5**

Hamamura Y, Saito C, Awai C, Kurihara D, Miyawaki A, Nakagawa T, Kanaoka MM, Sasaki N, Nakano A, Berger F, Higashiyama T (2011) Live-Cell Imaging Reveals the Dynamics of Two Sperm Cells during Double Fertilization in *Arabidopsis thaliana*. Curr Biol **21**: 497–502

Haughn G, Chaudhury A (2005) Genetic analysis of seed coat development in *Arabidopsis*. Trends Plant Sci **10**: 472–477

Higashiyama T (2010) Peptide signaling in pollen-pistil interactions. Plant Cell Physiol **51**: 177–189

Higashiyama T, Kuroiwa H, Kuroiwa T (2003) Pollen-tube guidance: beacons from the female gametophyte. Curr Opin Plant Biol **6**: 36–41

Higashiyama T, Yabe S, Sasaki N, Nishimura Y, Miyagishima S, Kuroiwa H, Kuroiwa T (2001) Pollen tube attraction by the synergid cell. Science **293**: 1480–1483

Higashiyama T, Yang W (2017) Gametophytic Pollen Tube Guidance: Attractant Peptides, Gametic Controls, and Receptors. Plant Physiol **173**: 112-121

Huang Q, Dresselhaus T, Gu H, Qu LJ (2015) Active role of small peptides in *Arabidopsis* reproduction: expression evidence. J Integr Plant Biol **57**: 518–521

Hülskamp M, Schneitz K, Pruitt RE (1995) Genetic Evidence for a Long-Range Activity That Directs Pollen Tube Guidance in *Arabidopsis*. Plant Cell **7**: 57-64

Jacob Y, Mongkolsiriwatana C, Veley KM, Kim SY, Michaels SD (2007) The Nuclear Pore Protein AtTPR Is Required for RNA Homeostasis, Flowering Time, and Auxin Signaling. Plant Physiol **144**: 1383–1390

Kadokura S, Sugimoto K, Tarr P, Suzuki T, Matsunaga S (2018) Characterization of somatic embryogenesis initiated from the *Arabidopsis* shoot apex. Dev Bio

Kanaoka MM, Kawano N, Matsubara Y, Susaki D, Okuda S, Sasaki N, Higashiyama T (2011) Identification and characterization of *TcCRP1*, a pollen tube attractant from *Torenia concolor*. Ann Bot (Lond) **108**: 739–747

Kawano N, Susaki D, Sasaki N, Higashiyama T, Kanaoka MM (2011) Isolation of Gametophytic Cells and Identification of Their Cell-Specific Markers in *Torenia fournieri*, *T. concolor* and *Lindernia micrantha*. Cytologia **76**: 177-184

Kelley DR, Gasser CS (2009) Ovule development: genetic trends and evolutionary considerations. Sex Plant Reprod **22**: 229–234

Khan D, Millar JL, Girard IJ, Chan A, Kirkbride RC, Pelletier JM, Kost S, Becker MG, Yeung EC, Stasolla C, Goldberg RB, Harada JJ, Belmonte MF (2015) Transcriptome

atlas of the *Arabidopsis* funiculus - a study of maternal seed subregions. Plant J **82**: 41-53

Kieber JJ, Ecker JR (1994) Molecular and genetic analysis of the constitutive ethylene response mutation ctr1. In: Coruzzi G, Puigdomenech P, Kieber JJ (eds) Plant molecular biology; molecular genetic analysis of plant development and metabolism. Springer-Verlag, Berlin, pp 193–201

Kieber JJ, Rothenberg M, Roman G, Feldman KA, Ecker JR (1993) *CTR1*, a negative regulator of the ethylene response pathway in *Arabidopsis*, encodes a member of the Raf family of protein kinases. Cell **72**: 427–441

Klepikova AV, Kasianov AS, Gerasimov ES, Logacheva MD, Penin AA (2016) A high resolution map of the *Arabidopsis thaliana* developmental transcriptome based on RNA-seq profiling. Plant J **88**: 1058–1070

Kumpf RP, Shi C-L, Larrieu A, Sto IM, Butenko MA, Peret B, Riiser ES, Bennett MJ, Aalen RB (2013) Floral organ abscission peptide IDA and its HAE/HSL2 receptors control cell separation during lateral root emergence. Proc Natl Acad Sci **110**: 5235–5240

Kurihara D, Mizuta Y, Sato Y, Higashiyama T (2015) ClearSee: a rapid optical clearing reagent for whole-plant fluorescence imaging. Development **142**: 4168-4179

Lafon-Placette C, Köhler C (2014) Embryo and endosperm, partners in seed development. Curr Opin Plant Biol **17**: 64-69

Larsson E, Vivian-Smith A, Offringa R, Sundberg E (2017) Auxin Homeostasis in *Arabidopsis* Ovules Is Anther-Dependent at Maturation and Changes Dynamically upon Fertilization. Front Plant Sci **8**

Lewis MW, Leslie ME, Liljegren SJ (2006) Plant separation: 50 ways to leave your mother. Curr Opin Plant Biol **9**: 59-65

Li C, Wu H, Cheung AY (2016) FERONIA and her pals: Functions and mechanisms. Plant Physiol **171**: 2379–2392

Lora J, Hormaza, JI, Herrero M (2016) The Diversity of the Pollen Tube Pathway in Plants: Toward an Increasing Control by the Sporophyte. Front Plant Sci **7**: 107

Loureiro J, Rodriguez E, Doležel J, Santos C (2007) Two New Nuclear Isolation Buffers for Plant DNA Flow Cytometry: A Test with 37 Species. Ann Bot **100**: 875–888

Luo M, Bilodeau P, Dennis ES, Peacock J, Chaudhury A (2000) Expression and Parent-of-Origin Effects for *FIS2*, *MEA*, and *FIE* in the Endosperm and Embryo of Developing *Arabidopsis* Seeds. Proc Natl Acad Sci USA **97**: 10637–10642

Ma H, Yanofsky M F, Meyerowitz EM (1991) *AGL1-AGL6*, an *Arabidopsis* gene family with similarity to floral homeotic and transcription factor genes. Genes Dev **5**: 484–495

Maheshwari P (1950) An Introduction to the Embryology of Angiosperms. (New York: McGraw-Hill)

Mawson BT, Steghaus AK, Yeung EC (1994) Structural development and respiratory activity of the funiculus during bean seed (*Phaseolus vulgaris L.*) maturation. Ann Bot **74**: 587–594

McCormick S (2004) Control of male gametophyte development. Plant Cell **16**: S142-S153

Mecchia MA, Santos-Fernandez G, Duss NN, Somoza SC, Boisson-Dernier A, Gagliardini V, Martinez-Bernardini A, Fabrice TN, Ringli C, Muschietti JP, Grossniklaus U (2017) RALF4/19 peptides interact with LRX proteins to control pollen tube growth in *Arabidopsis*. Science **358**: 1600-1603

Meng X, Zhou J, Tang J, Li B, De Oliveira M, Chai J, He P, Shan L (2016) Ligand-Induced Receptor-like Kinase Complex Regulates Floral Organ Abscission in *Arabidopsis*. Cell Rep **14**: 1330-1338

Miyazaki S, Murata T, Sakurai-Ozato N, Kubo M, Demura T, Fukuda H, Hasebe M (2009) *ANXUR1* and *2*, Sister Genes to *FERONIA/SIRENE*, Are Male Factors for Coordinated Fertilization. Curr Biol **19**: 1327-1331

Mizzotti C, Ezquer I, Paolo D, Rueda-Romero P, Guerra RF, Battaglia R, Rogachev I, Aharoni A, Kater MM, Caporali E, Colombo L (2014) SEEDSTICK is a Master Regulator of Development and Metabolism in the *Arabidopsis* Seed Coat. PLoS Genet **10**: e1004856

Mizzotti C, Mendes MA, Caporali E, Schnittger A, Kater MM, Battaglia R, Colombo L (2012) The MADS box genes *SEEDSTICK* and *ARABIDOPSIS Bsister* play a maternal role in fertilization and seed development. Plant J **70**: 409–420

Moïse JA, Han S, Gudynaitï-Savitch L, Johnson DA, Miki BLA (2005) Seed coats: structure, development, composition, and biotechnology. In Vitro Cell Dev Biol Plant **41**: 620–644

Murphy E, Smet ID (2014) Understanding the RALF family: A tale of many species. Trends Plant Sci **19**: 664-671

Musielak T, Bürgel P, Kolb M, Bayer M (2016) Use of SCRI Renaissance 2200 (SR2200) as a Versatile Dye for Imaging of Developing Embryos, Whole Ovules, Pollen Tubes and Roots. Bio-Protocol **6**

Musielak T, Schenkel L, Kolb M, Henschen A, Bayer M (2015) A simple and versatile cell wall staining protocol to study plant reproduction. Plant Reprod **28**: 161–169

Nesi N, Debeaujon I, Jond C, Stewart AJ, Jenkins GI, Caboche M, Lepiniec L (2002) The *TRANSPARENT TESTA16* locus encodes the *ARABIDOPSIS BSISTER MADS* domain protein and is required for proper development and pigmentation of the seed coat. Plant Cell **14**: 2463–2479

Nole-Wilson S, Azhakanandam S, Franks RG (2010) Polar auxin transport together with *AINTEGUMENTA* and *REVOLUTA* coordinate early *Arabidopsis* gynoecium development. Dev Biol **346**: 181–195

Nowack MK, Ungru A, Bjerkan KN, Grini PE, Schnittger A (2010) Reproductive cross-talk: seed development in flowering plants. Biochem Soc Trans **38**: 604–612

Okuda S, Tsutsui H, Shiina K, Sprunck S, Takeuchi H, Yui R, Kasahara RD, Hamamura Y, Mizukami A, Susaki D, Kawano N, Sakakibara T, Namiki S, Itoh K, Otsuka K, Matsuzaki M, Nozaki H, Kuroiwa T, Nakano A, Kanaoka MM, Dresselhaus T, Sasaki N, Higashiyama T (2009) Defensin-like polypeptide LUREs are pollen tube attractants secreted from synergid cells. Nature **458**: 357–361

Palanivelu R, Tsukamoto T (2012) Pathfinding in angiosperm reproduction: pollen tube guidance by pistils ensures successful double fertilization. WIREs Dev Biol **1**: 96–113

Park K, Frost JM, Adair AJ, Kim DM, Yun H, Brooks JS, Fischer RL, Choi Y (2016) Optimized Methods for the Isolation of *Arabidopsis* Female Central Cells and Their Nuclei. Mol Cells **39**: 768–775

Pereira AM, Masiero S, Nobre MS, Costa ML, Solís M-T, Testillano PS, Sprunck S, Coimbra S (2014) Differential expression patterns of Arabinogalactan Proteins in *Arabidopsis thaliana* reproductive tissues. J Exp Bot **65**: 5459–5471

Pereira AM, Nobre MS, Pinto SC, Lopes AL, Costa ML, Masiero S, Coimbra S (2016) "Love is strong, and you're so sweet": JAGGER is essential for persistent synergid degeneration and polytubey block in *Arabidopsis thaliana*. Mol Plant **9**: 601–614

Pillitteri LJ, Bemis SM, Shpak ED, Torii KU (2007) Haploinsufficiency after successive loss of signaling reveals a role for ERECTA-family genes in *Arabidopsis* ovule development. Development **134**: 3099–3109

Pinyopich A, Ditta GS, Savidge B, Liljegren SJ, Baumann E, Wisman E, Yanofsky MF (2003) Assessing the redundancy of MADS-box genes during carpel and ovule development. Nature **424**: 85–88

Qu LJ, Li L, Lan Z, Dresselhaus T (2015) Peptide Signalling during the Pollen Tube Journey and Double Fertilization. J Exp Bot **66**: 5139–5150

Raghavan V (2003) Some reflections on double fertilization, from its discovery to the present. New Phytol **159**: 565–583

Reiser L, Modrusan Z, Margossian L, Samach A, Ohad N, Haughn GW, Fischer RL (1995) The *BELL1* gene encodes a homeodomain protein involved in pattern formation in the *Arabidopsis* ovule primordium. Cell **83**: 735–742

Robinson-Beers K, Pruitt RE, Gasser CS (1992). Ovule development in wild-type *Arabidopsis* and two female-sterile mutants. Plant Cell **4**: 1237–1249

Rottmann TM, Fritz C, Lauter A, Schneider S, Fischer C, Danzberger N, Dietrich P, Sauer N, Stadler R (2018) Protoplast-Esculin Assay as a New Method to Assay Plant Sucrose Transporters: Characterization of *AtSUC6* and *AtSUC7* Sucrose Uptake Activity in *Arabidopsis* Col-0 Ecotype. Front Plant Sci **9**: 430

Savidge B, Rounsley SD, Yanofsky MF (1995) Temporal relationship between the transcription of two *Arabidopsis* MADS box genes and the floral organ identity genes. Plant Cell **7**: 721–733

Schneider CA, Rasband WS, Eliceiri KW (2012) NIH Image to ImageJ: 25 years of image analysis. Nat Methods **9**: 671–675

Schneitz K, Hülskamp M, Pruitt RE (1995) Wild-type ovule development in *Arabidopsis thaliana*: a light microscope study of cleared whole-mount tissue. Plant J **7**: 731–749

Schroeder A, Mueller O, Stocker S, Salowsky R, Leiber M, Gassmann M, Lightfoot S, Menzel W, Granzow M, Ragg T (2006) The RIN: an RNA integrity number for assigning integrity values to RNA measurements. BMC Mol Biol **7**: 3

Shimizu KK, Okada K (2000) Attractive and repulsive interactions between female and male gametophytes in *Arabidopsis* pollen tube guidance. Development **127**: 4511–4518

Silverstein KA, Moskal WA Jr, Wu HC, Underwood BA, Graham MA, Town CD, VandenBosch KA (2007) Small cysteine-rich peptides resembling antimicrobial peptides have been under-predicted in plants. Plant J **51**: 262–80

Smyth DR, **Bowman JL**, **Meyerowitz EM** (1990) Early flower development in *Arabidopsis*. Plant Cell **2**: 755–767

Stepanova AN, Robertson-Hoyt J, Yun J, Benavente LM, Xie D, Dolezal K, Schlereth A, Jurgens G, Alonso JM (2008) TAA1-mediated auxin biosynthesis is essential for hormone crosstalk and plant development. Cell **133**:177–191

Suzuki T, Fujikura K, Higashiyama T, Takata K (1997) DNA staining for fluorescence and laser confocal microscopy. J Histochem Cytochem **45**: 49–53

Takeuchi H, Higashiyama T (2012) A species-specific cluster of defensin-like genes encodes diffusible pollen tube attractants in *Arabidopsis*. PLoS Biol **10**: e1001449

Takeuchi H, Higashiyama T (2016) Tip-localized receptors control pollen tube growth and LURE sensing in *Arabidopsis*. Nature **531**: 245–248

Tao Y, Ferrer JL, Ljung K, Pojer F, Hong F, Long JA, Li L, Moreno JE, Bowman ME, Ivans LJ, Cheng Y, Lim J, Zhao Y, Ballare CL, Sandberg G, Noel JP, Chory J (2008)

Rapid synthesis of auxin via a new tryptophan-dependent pathway is required for shade avoidance in plants. Cell **133**:164–176

Tsai AY, Kunieda T, Rogalski J, Foster LJ, Ellis BE, Haughn GW (2016) Identification and Characterization of *Arabidopsis* Seed Coat Mucilage Proteins. Plant Physiol **173**: 1059-1074

Tung C-W, Dwyer KG, Nasrallah ME, Nasrallah JB (2005) Genome-Wide Identification of Genes Expressed in *Arabidopsis* Pistils Specifically along the Path of Pollen Tube Growth. Plant Physiol **138**: 977-989

Vanoosthuyse V, Miège C, Dumas C, Cock JM (2001) Two large *Arabidopsis thaliana* gene families are homologous to the Brassica gene superfamily that encodes pollen coat proteins and the male component of the self-incompatibility response. Plant Mol Biol **46**: 17-34

Villanueva JM, Broadhvest J, Hauser BA, Meister RJ, Schneitz K, Gasser CS (1999) INNER NO OUTER regulates abaxial – adaxial patterning in *Arabidopsis* ovules. Gene Dev **13**: 3160–3169

Wang P, Hawkins TJ, Richardson C, Cummins I, Deeks MJ, Sparkes I, Hawes C, Hussey PJ (2014) The plant cytoskeleton, NET3C, and VAP27 mediate the link between the plasma membrane and endoplasmic reticulum. Curr Biol **24**: 1397-1405

Wang T, Liang L, Xue Y, Jia PF, Chen W, Zhang MX, Wang YC, Li HJ, Yang WC (2016) A receptor heteromer mediates the male perception of female attractants in plants. Nature **531**: 241–244

Wang Y, Zhang W, Song L, Zou J, Su Z, Wu W (2008) Transcriptome Analyses Show Changes in Gene Expression to Accompany Pollen Germination and Tube Growth in *Arabidopsis*. Plant Physiol **148**: 1201-1211

Wen J, Li J, Walker JC (2012) Overexpression of a serine carboxypeptidase increases carpel number and seed production in *Arabidopsis thaliana*. Food and Energy Security **1**: 61-69

Yadegari R, Drews GN (2004) Female gametophyte development. Plant Cell **16**: S133-S141

Yan W, Chen D, Kaufmann K (2016) Molecular mechanisms of floral organ specification by MADS domain proteins. Curr Opin Plant Biol **29**: 154–162

Yoo SD, Cho YH, Sheen J (2007) *Arabidopsis* mesophyll protoplasts: a versatile cell system for transient gene expression analysis. Nat Protoc **2**: 1565–1572

Zhai Z, Jung H, Vatamaniuk OK (2009) Isolation of Protoplasts from Tissues of 14-day-old Seedlings of *Arabidopsis thaliana*. J Vis Exp pp 1149

Zhang C, Barthelson RA, Lambert GM, Galbraith DW (2008) Global Characterization of Cell-Specific Gene Expression through Fluorescence-Activated Sorting of Nuclei. Plant Physiol **147**: 30–40

7. Supplemental material

Supplemental Table 1. List of primers used for genotyping and cDNA validation by RT-PCR. cDNA- complementary DNA; gDNA- genomic DNA; mt- mutant DNA; WT- wild type DNA.

Gene	AGI code	Primer name	Sequence	Product size (bp)	Purpose
STK	*AT4G09960*	STK_FW STK_RV	GCTTGTTCTGATAGCACCAACACTAGCA GGAACTCAAAGAGTCTCCCATCAG	350 (WT) 400 (mt)	Genotyping *stk*
AGP9	*AT2G14890*	AGP9_FW AGP9_RV	CTCTAGCTTCCCCTCCTGCT AAGCTCGAAACCATCTTGCT	197 (cDNA) 1046 (gDNA)	RT-PCR
AGP4	*AT5G10430*	AGP4_FW AGP4_RV	TTGCTCCTTCTCCTGCTGAT AACGGCGGCGTACATAATAG	176 (cDNA/ gDNA)	RT-PCR
SUS4	*AT3G43190*	SUS4_FW SUS4_RV	CAACACCACCAGATCATTGC TGACCACCTGTGTCAGGGTA	779 (cDNA) 942 (gDNA)	RT-PCR
FIS2	*AT2G35670*	FIS2_FW FIS2_RV	AGCGTCTTAAGGGTCGACAG GATTGTTGGCATTAGCAGCA	441(cDNA) 881 (gDNA)	RT-PCR
ACT7	*AT5G09810*	ACT7_FW ACT7_RV	GGCCGATGGTGAGGATATTCAGCCACTTG TCGATGGACCTGACTCATCGTACTCACTC	1109 (cDNA) 1387 (gDNA)	RT-PCR

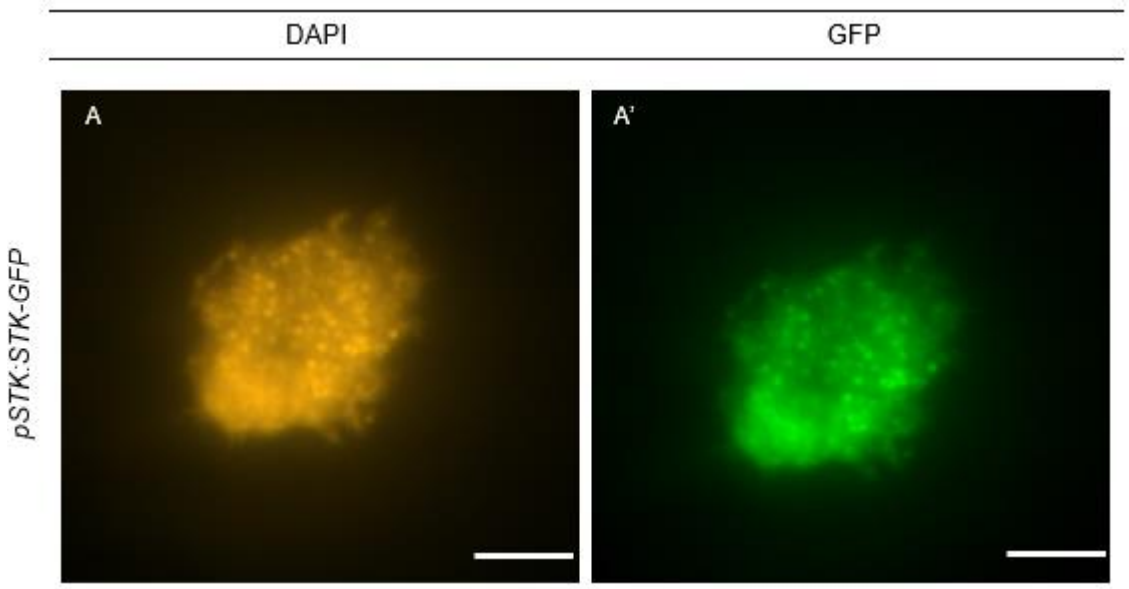

Supplemental Figure 1. Nuclei isolation of *A. thaliana* fixed ovules from *pSTK:STK-GFP* line. *pSTK:STK-GFP* stage 12 ovules (according to Smyth *et al.*, 1990) were used. Nuclei isolation was checked under the fluorescent microscope using DAPI **(A)** and GFP channel **(A')**. It was observed many dots with emission of DAPI and GFP signal. Scale bars = 50 µm.

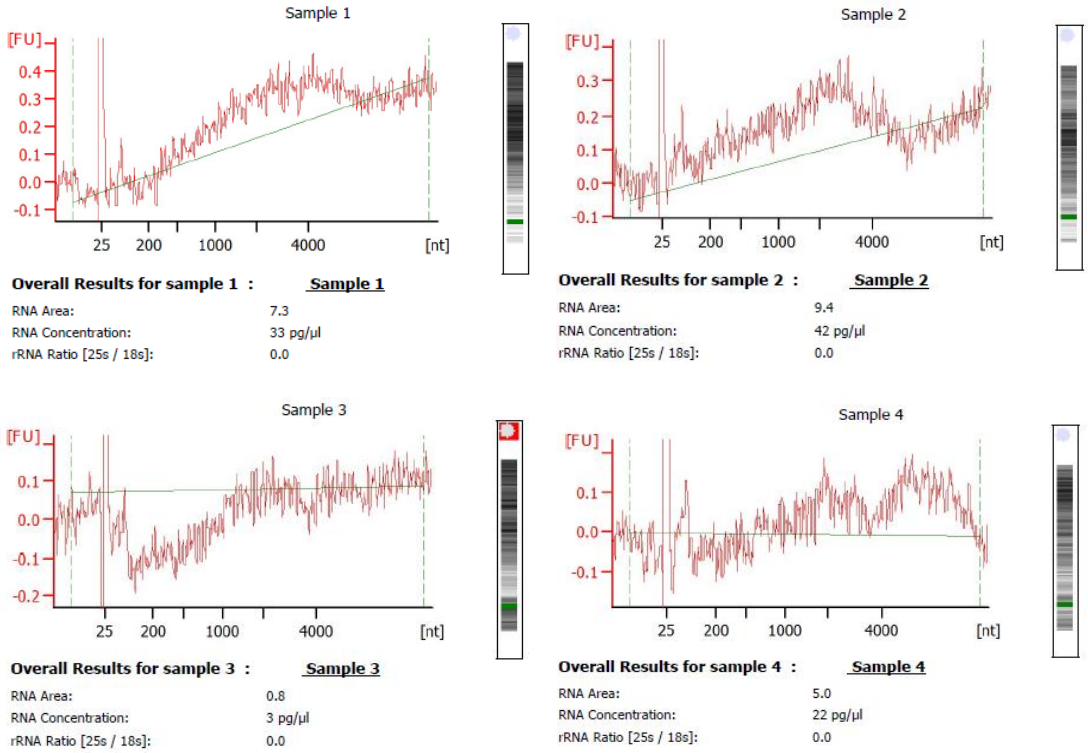

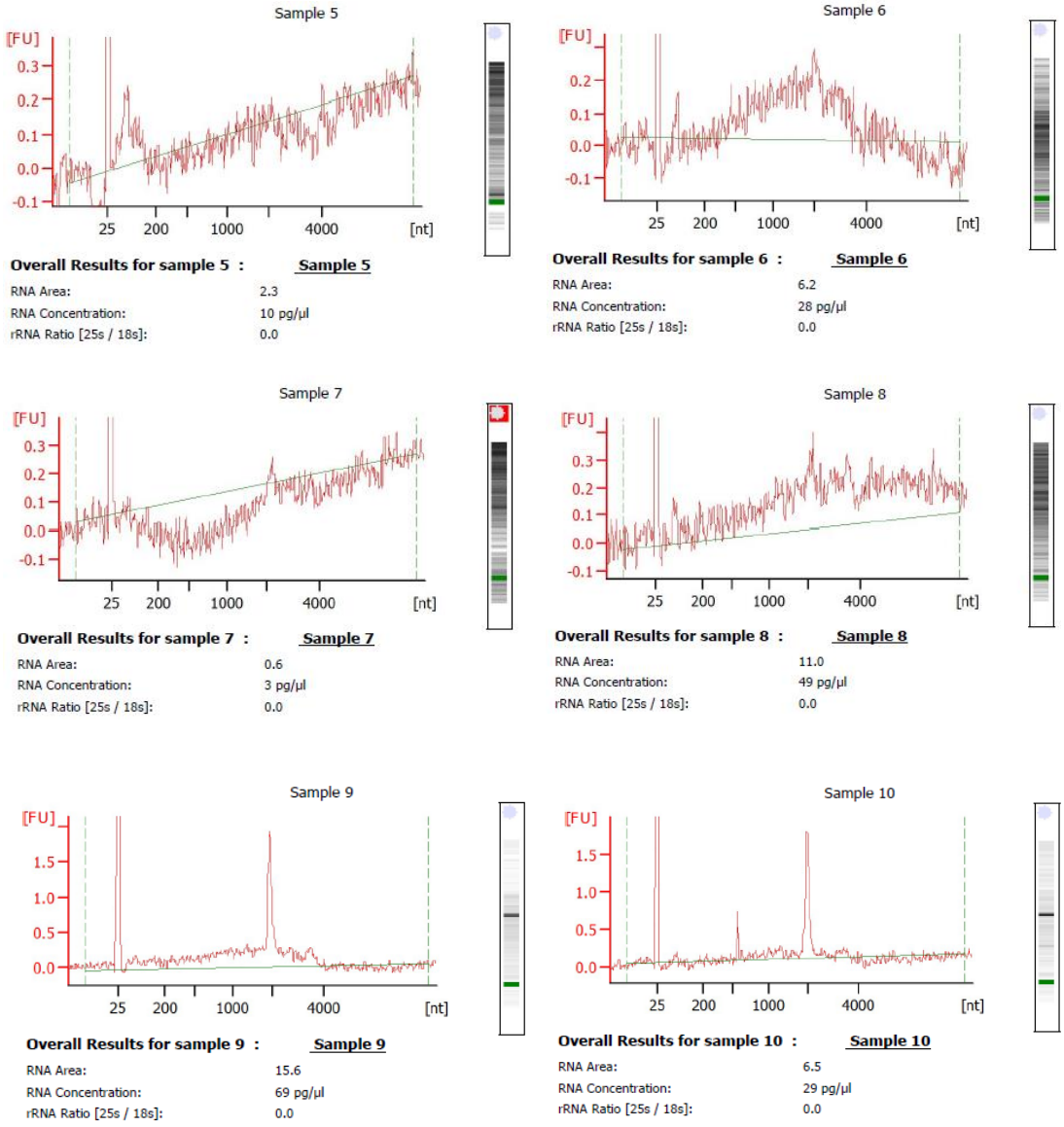

Supplemental Figure 2. Electropherogram of mRNA samples. Samples 1, 2, 4, 5, and 7 represent mRNA extracted from 10, 40, 35, 20 and 50 funiculi, respectively. Sample 9 contains ovules from 5 pistils. Samples 3, 6, 8 and 10 are replicates of samples 2, 5, 7 and 9, respectively. All the biological material used are from flowers at stage 12 (according to Smyth *et al.*, 1990). Overall, no contamination from rRNA was detected on the mRNA samples.

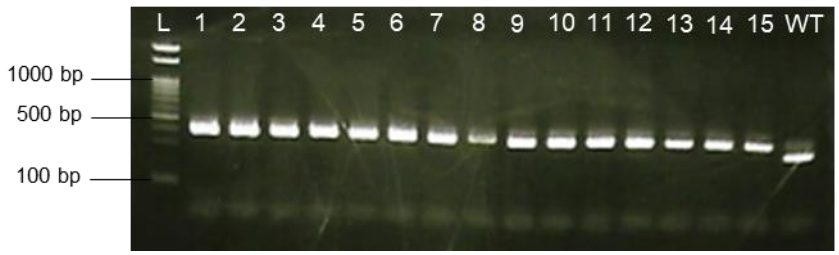

Supplemental Figure 3. Electrophoretic analysis of gDNA fragments corresponding to *stk* genotyping. 350 bp and 400 bp are the expected size of fragments from wild type and mutant plants, respectively. 1-15 represent samples from the plants analysed; WT stands for gDNA extracted from wild type plants; L– Molecular DNA weight ladder.